Georgia Institute of Technology

School of Civil and Environmental Engineering

Structural Engineering, Mechanics and Materials
Research Report No. 02-3

Strengthening of Reinforced Concrete Bridge Deck Slabs with Shop-Manufactured Carbon Composite Plates

Prepared for

Georgia Department of Transportation
Federal Highway Administration

GDOT Research Project No. GDOT R.P. 9702

by

A. Zureick, L. F. Kahn and Y. S. Kim

February 2002

TECHNICAL REPORT DOCUMENTATION PAGE

1. Report No. (FHWA-RD-95-###)	2. Government Accession No.	3. Recipient's Catalog No.
4. Title Strengthening of Reinforced Concrete Bridge Deck Slabs with Shop-Manufactured Carbon Composite Plates		5. Report Date: 6. Performing Organization Code:
7. Author(s) A. Zureick, L. F. Kahn, and Y. S. Kim		8. Performing Organization Rpt. No.
9. Performing Organization Name and Address: Georgia Institute of Technology Structural Engineering, Mechanics, and Materials School of Civil and Environmental Engineering Atlanta, GA 30332-0355		10. Work Unit No. (TRAIS) (NCP number goes here) 11. Contract or Grant No.
12. Sponsoring Agency Name and Address Georgia Department of Transportation Federal Highway Administration		13. Type of Report / Period Covered 14. Sponsoring Agency Code

15. Supplementary Notes
Contracting Officer's Technical Representative (COTR) -- name of FHWA staff member, routing code)

16. Abstract

This report examines the performance of reinforced concrete bridge deck slabs externally strengthened using carbon fiber reinforced polymer (CFRP) composite plates shop-manufactured by the pultrusion process. Eleven full-scale reinforced concrete bridge deck specimens were constructed with 3,640 psi and 3,840 psi concrete and were reinforced with number 5 steel reinforcing bars near the top and bottom surface. Five specimens were subjected to two loading cycles. In the first cycle, the specimens were loaded until significant cracks were developed and the tensile reinforcing steel yielded. The specimens were then strengthened with carbon FRP composite plates. The second loading cycle was applied until failure of the deck specimens occurred. Six specimens were strengthened before cracking and then loaded to failure. The average ultimate strength increased by 30% after rehabilitation or strengthening. This increase was attained after allowing the epoxy adhesive to cure at least 10 days.

17. Key Words	18. Distribution Statement		
Rehabilitation, strengthening, polymer, carbon fibers, composites, Testing			
19. Security Classif. (of this report)	20. Security Classif. (of this page)	21. No. of Pages (inc. front matter)	22. Price

SI* (MODERN METRIC) CONVERSION FACTORS

APPROXIMATE CONVERSIONS TO SI UNITS

Symbol	When You Know	Multiply By	To Find	Symbol
		LENGTH		
in	inches	25.4	millimeters	mm
ft	feet	0.305	meters	m
yd	yards	0.914	meters	m
mi	miles	1.61	kilometers	km
		AREA		
in^2	square inches	645.2	square millimeters	mm^2
ft^2	square feet	0.093	square meters	m^2
yd^2	square yards	0.836	square meters	m^2
ac	acres	0.405	hectares	ha
mi^2	square miles	2.59	square kilometers	km^2
		VOLUME		
fl. oz.	fluid ounces	29.57	milliliters	ml
gal	gallons	3.785	liters	l
ft^3	cubic feet	0.028	cubic meters	m^3
yd^3	cubic yards	0.765	cubic meters	m^3
	NOTE: Volumes greater than 1000 l shall be shown in m^3			
		MASS		
oz	ounces	28.35	grams	g
lb	pounds	0.454	kilograms	kg
T	short tons (2000 lbs)	0.907	megagrams	Mg
		TEMPERATURE (exact)		
°F	Fahrenheit temperature	5 (F-32)/9 or (F-32)/1.8	Celsius temperature	°C
		ILLUMINATION		
fc	foot-candles	10.76	lux	lx
fl	foot-Lamberts	3.426	candela/m^2	cd/m^2
		FORCE and PRESSURE or STRESS		
lbf	poundforce	4.45	newtons	N
psi	poundforce per square inch	6.89	kilopascals	kPa

APPROXIMATE CONVERSIONS FROM SI UNITS

Symbol	When You Know	Multiply By	To Find	Symbol
		LENGTH		
mm	millimeters	0.039	inches	in
m	meters	3.28	feet	ft
m	meters	1.09	yards	yd
km	kilometers	0.621	miles	mi
		AREA		
mm^2	square millimeters	0.0016	square inches	in^2
m^2	square meters	10.764	square feet	ft^2
m^2	square meters	1.195	square yards	yd^2
ha	hectares	2.47	acres	ac
km^2	square kilometers	0.386	square miles	mi^2
		VOLUME		
ml	milliliters	0.034	fluid ounces	fl. oz.
l	liters	0.264	gallons	gal.
m^3	cubic meters	35.71	cubic feet	ft^3
m^3	cubic meters	1.307	cubic yards	yd^3
		MASS		
g	grams	0.035	ounces	oz
kg	kilograms	2.202	pounds	lb
Mg	megagrams	1.103	short tons (2000 lb)	T
		TEMPERATURE (exact)		
°C	Celsius temperature	1.8C + 32	Fahrenheit temperature	°F
		ILLUMINATION		
lx	lux	0.0929	foot-candles	fc
cd/m^2	candela/m^2	0.2919	foot-Lamberts	fl
		FORCE and PRESSURE or STRESS		
N	newtons	0.225	poundforce	lbf
kPa	kilopascals	0.145	poundforce per square inch	psi

*SI is the symbol for the International System of Units. Appropriate rounding should be made to comply with Section 4 of ASTM E380.

(Revised August 1992)

TABLE OF CONTENTS

LIST OF TABLES

LIST OF FIGURES

CHAPTER I TEST PROGRAM

Introduction

Fiber-reinforced polymer (FRP) composite materials provide an alternative technique for rehabilitating and strengthening existing reinforced and prestressed concrete bridge components. Whether a component has been damaged due to overload, earthquake or material deterioration or whether the structure requires strengthening to resist increased future live loads, wind or seismic forces, FRPs provide an efficient, cost-effective and easy-to-construct means to reinforce concrete members. They may be placed with less disturbance to bridge traffic and other functions as compared to rehabilitation using additional steel reinforcement.

The concept of strengthening with FRP was pioneered by Professor U. Meier, at the Swiss Federal Laboratories for Materials Testing and Research Institute in the early 1980's. His extensive research activities lead to the first-time field implementation of FRP rehabilitation for both bridge and building applications. Both the Ibach bridge near Lucern, Switzerland, and the City Hall of Gossau St. Gall in northeaster Switzerland were strengthened in 1991 by bonding pultruded carbon fiber polymer plates to the exterior surfaces of the concrete structures. Details on some of these and other early applications are described by Meier et al. (1993). Since then, there has been a worldwide keen interest not only to utilize polymeric materials in strengthening structures but also to examine the materials' structural behavior under a variety of loading and environmental conditions. While a review highlighting some fundamental concepts pertaining to the use of FRP materials in structural rehabilitation is found in an article by Triantafillou (1998), comprehensive expositions of past research activities, test results, and case studies on the same subject are given in a recent monograph by Hollaway and Leeming (1999).

Purpose, Objectives and Research Significance

The purpose of this experimental research was to determine the effectiveness of strengthening existing reinforced concrete bridge decks with shop-manufactured carbon fiber reinforced polymer (CFRP) plates. Specific objectives included determining the strength increase provided when various amounts of CFRP plates were bonded to the tension face of bridge deck speci-

mens, identifying the failure mode of strengthened bridge decks, determining if the presence of an existing crack influenced the bond and failure of CFRP plates, experimentally determining the strength reduction due to misalignment of CFRP plates, and the adhesive ambient temperature curing time required to attain such strengths.

Test Specimens

Eleven reinforced concrete bridge deck slab specimens 10 feet long by 3 feet wide and 7 inches thick were constructed using a normal weight, 3,640 psi or 3,840 psi concrete to mimic standard highway bridge decks. The slab specimens were cast in two groups. The first group consisted of five specimens, which were first tested in the as-built (non-rehabilitated) condition, then they were strengthened using carbon composite plates and retested. These first five specimens were labeled RH-1 to RH-5. After rehabilitation and strengthening they were labeled RH-1R to RH-5R. The second group consisted of six specimens strengthened with carbon composite plates before testing. These six specimens were labeled ST-1 to ST-6. The steel reinforcement scheme in all specimens consisted of top and bottom longitudinal layers of Grade 60, number 5 steel reinforcing bars with transverse top and bottom layers of number 4 bars as shown in Figure 1. The concrete cover for the bottom tension face was 1 inch, and the cover for the top reinforcement was 3.375 inches.

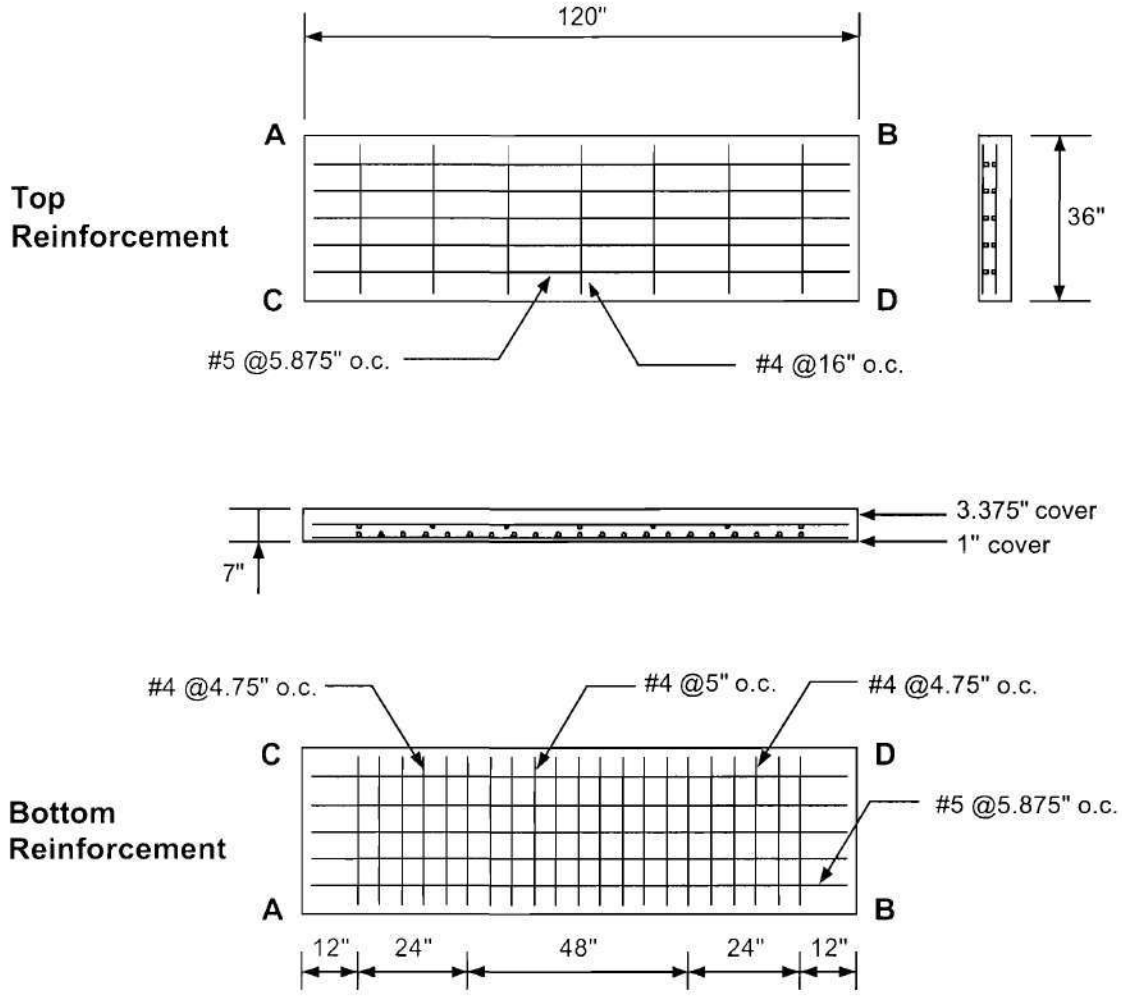

Figure 1. Specimen dimensions and steel layout

Loading

All deck specimens were tested with a span of 8 feet as illustrated in Figure 2. The loads were applied to the reinforced concrete slabs by a 140-kip closed loop hydraulic actuator mounted on a steel reaction frame shown in Figure 3. A 36 inch long, 4 inch x 4 inch x 1/4 inch structural steel tube was used to distribute the load transversely from the actuator to the bridge deck specimens. A 1/4-inch thick neoprene pad was placed between the concrete and both the tube and the bearing plates to better distribute the load to the slightly irregular concrete surfaces. The loading and unloading rates for all specimens were 0.1 inch per minute.

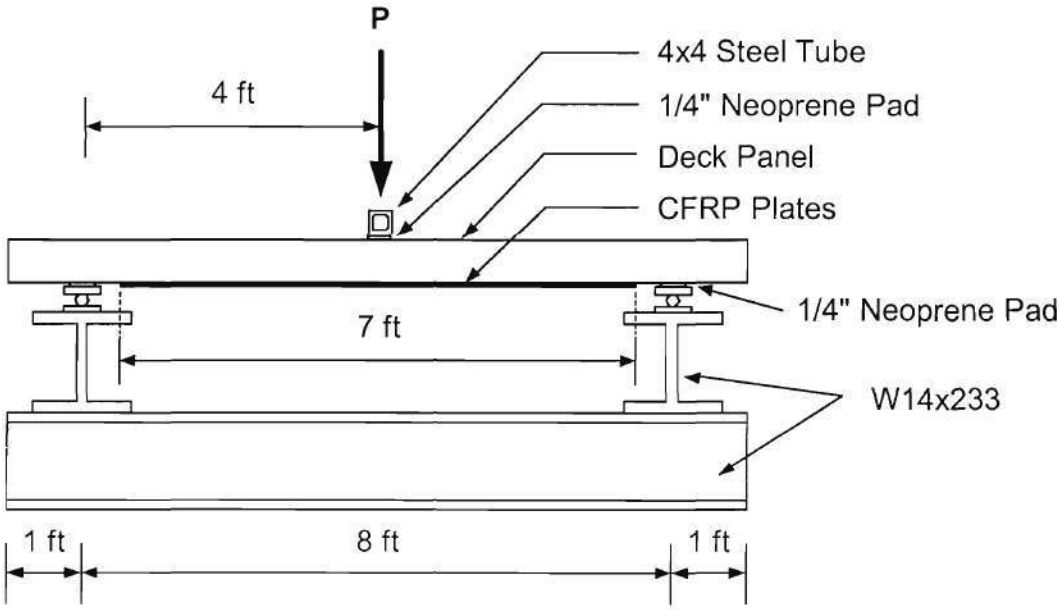

Figure 2. Typical test setup

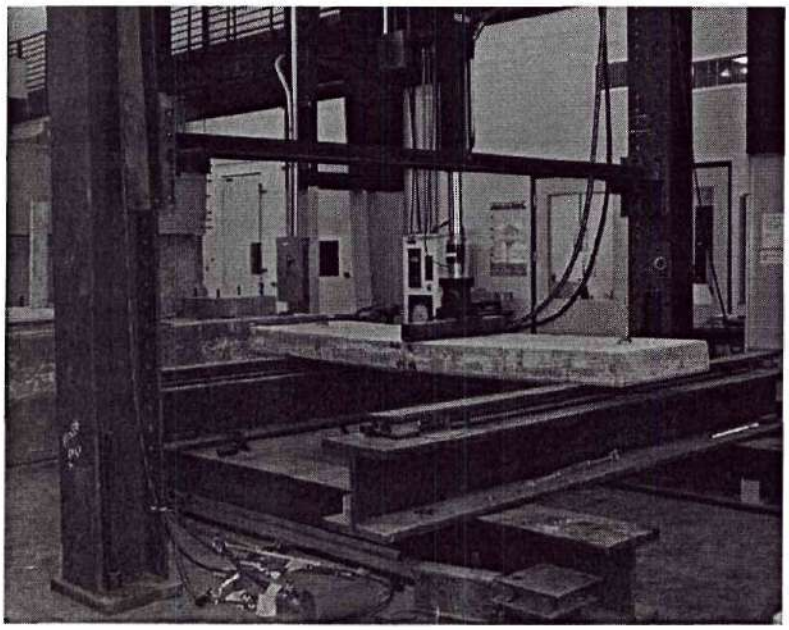

Figure 3. Photograph of test set-up

Instrumentation

Prior to the casting of the concrete, electrical resistant foil strain gages were mounted on the longitudinal reinforcing bars as shown in Figure 4. Because all specimens in each group used identical steel and concrete from the same batch, instrumenting three out of the five specimens in every group was deemed sufficient to understand the reinforcement behavior. For the first specimen (RH-1) all five bottom and five top steel bars were strain gaged at midspan. The second and third specimens (RH-2, RH-3) were equipped with three gages in both the top and bottom steel layers. Finally, the fourth and fifth specimens were not instrumented with strain gages. In Figure 4, the labeling on the left corresponds to the strain gages of RH-1 and the right-hand side labeling corresponds to the gages for RH-2 and RH-3. Three wire potentiometers located at the midspan were used to determine the vertical deflection of the bridge deck specimens as the load was applied as shown in Figure 4. Locating the deflection potentiometers transversely across the panel determined the uniformity of the deflection. It should be noted that the measured deflection from the potentiometers included small deflections resulting from the neoprene pads used between the concrete specimen and the supports. Loads were measured using a 110 kip load cell that was attached to the piston of the actuator. Crack widths were measured with a crack comparator.

Rehabilitated and strengthened slabs were instrumented with an additional set of 350-ohm electrical resistance strain gages and strain rosettes used to measure the strain in the carbon composite plates. Each specimen except ST-4, ST-5, and ST-6, had a strain gage placed on the center of each CFRP plate as shown in Figure 5. Specimens ST-4, ST-5, and ST-6 had a three-wire strain rosette on each CFRP plate with locations and orientations shown in the same Figure 5.

Load, deflection, reinforcing steel strain, and CFRP strains were obtained for both non-rehabilitated and rehabilitated tests and were collected using an Optim Megadac system and TCS for Windows software.

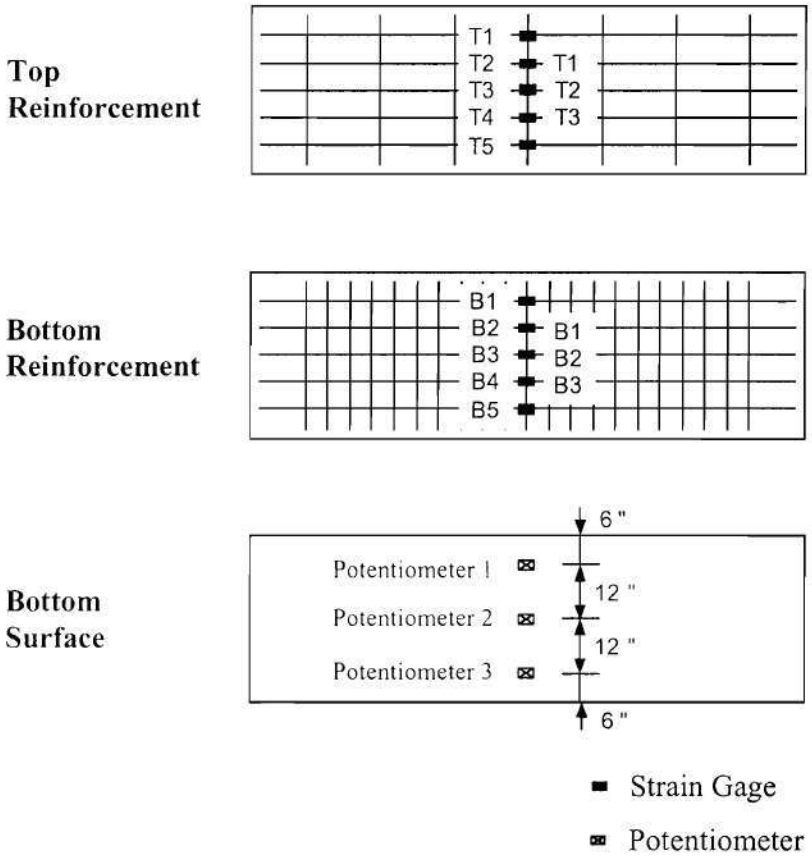

Figure 4. Location and labeling of strain gages and potentiometers

Deck Slabs RH-1R, RH-2R, RH-3R and ST-1, ST-2, ST-3

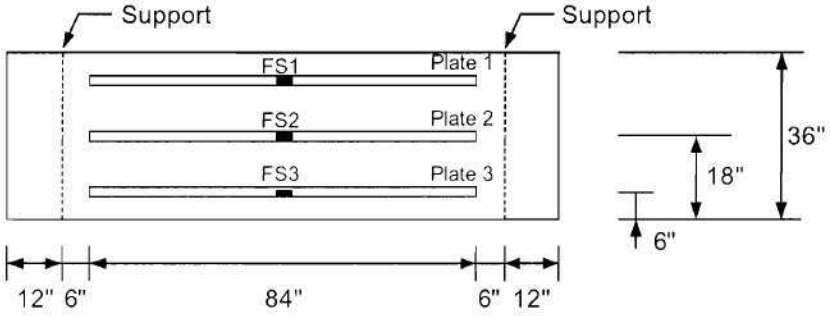

Deck Slabs RH-4R, RH-5R

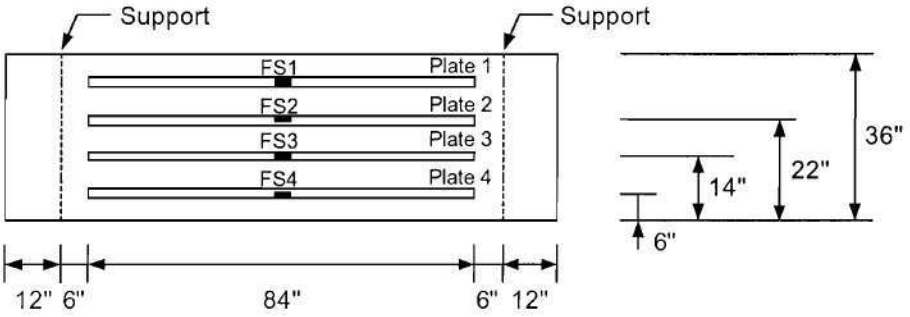

Deck Slabs ST-4, ST-5, ST-6

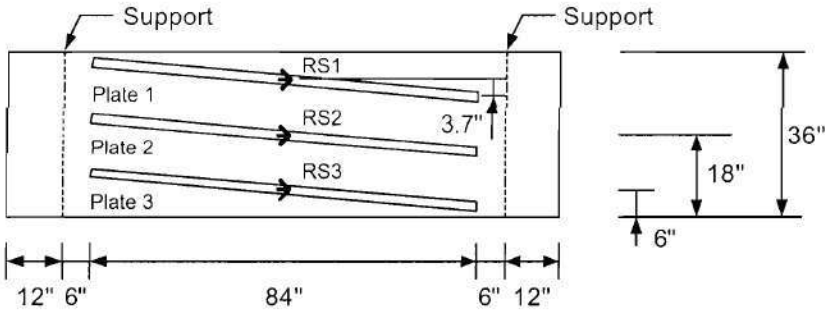

- Unidirectional Strain Gage
- Strain Rosette

Figure 5. CFRP plate layout on bottom surface of concrete specimens

CHAPTER II MATERIAL PROPERTIES

The reinforced concrete bridge deck slab specimens used in this investigation were cast in one group of five specimens and in a second group of six specimens. For each group forty concrete cylinders, 6-inch diameter and 12-inch long, were prepared for the determination of the concrete strength at 28 days and at the time of testing of each specimen. In addition, three 6" x 6" x 21" non-reinforced beams were cast for the determination of the modulus of rupture at age 28 days per ASTM C78. Table1 shows the results obtained for the compressive strength. This test date f'_c was used in all subsequent analyses.

Table 1. Concrete properties

Property		No. of Tests	Average Value (psi)	C.O.V. (%)
28-day Compressive Strength		6	2,754	7.2
Modulus of Rupture		3	578	3.0
Compressive Strength at the Time of Testing	RH-1, RH-2, RH-3	6	3,641	4.2
	RH-4, RH-5	6	3,834	5.3
	RH-1R ~ RH-5R	6	3,840	5.5
	ST-1 ~ ST-6	6	4,765	3.4

Six number 5 bars were tested to determine their actual yield stress. All specimens were reinforced with steel from the same batch. The average yield stress (f_y) was 72.6 ksi with a coefficient of variation equal to 2.5%, and the average elastic modulus (E_s) was 28,280 ksi.

Sika Carbodur® carbon plates were used to strengthen the slabs. The average width and thickness of these plates were 2 inches and 0.051 inch, respectively. Fifteen tensile coupons with nominal dimensions of 0.9 in. x 0.051 in. were tested in accordance with ASTM D3039 procedure. Results from these tests showed a variation in the strength ranging from 17.7 kips/in width to 22.1 kips/in width with an average value of 20 kips/in width and a coefficient of variation of 7.4 %. The strength of 20 kips/in width corresponds to an average stress of 196 ksi. Values of the ultimate tensile strain ranged from 1.41 % to 1.85 % with an average value of 1.6 % and a coefficient of variation of 8.2 %. The computed tensile modulus in the fiber direction showed very lit-

tle variations with an average value of 23,300 ksi. Figure 6 shows the stress-strain results for all 15 coupons; they indicate linear behavior throughout the test. Table 13 in the Appendix lists the results of all tests.

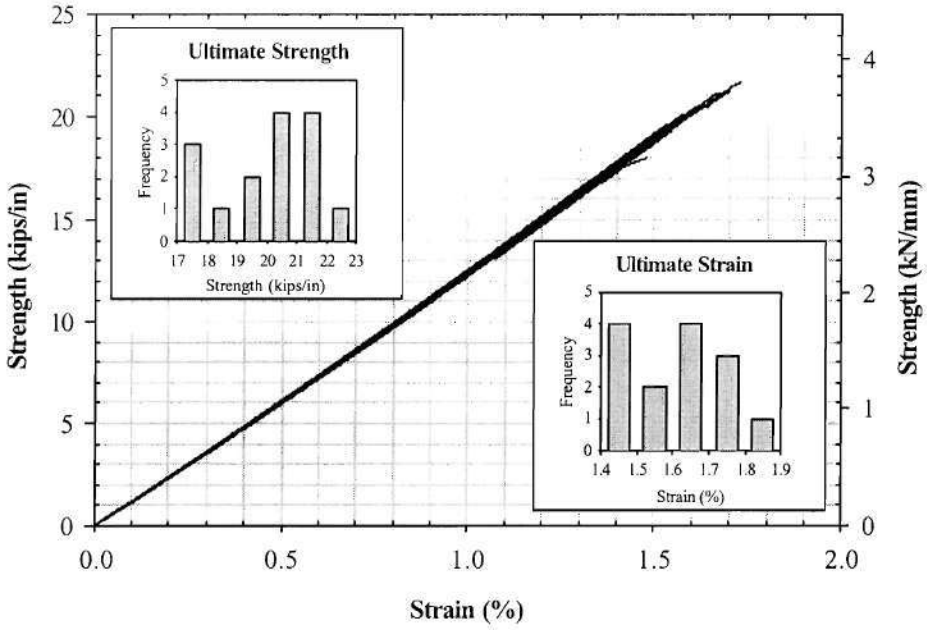

Figure 6. Stress-Strain diagram of Sika Carbodur® carbon plates

A room-temperature curing two part epoxy adhesive (Sikadur 30®) was used for bonding the CFRP plates to the concrete surface. Glass transition temperature (T_g) tests were conducted on adhesive specimens to examine the T_g variation with curing time over a range of temperatures between 20°C - 25°C. One sample per day was tested according to ASTM D3418. Tests were conducted over a period of one month at various intervals to study the variation over an extended time period. The results of the tests are depicted graphically in Figure 7.

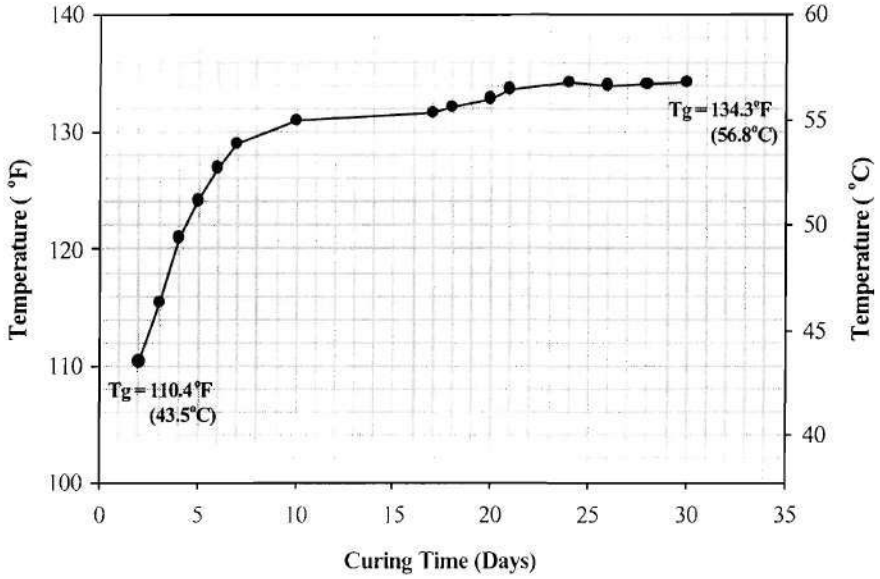

Figure 7. Variation of glass transition temperature with curing time

The response of the adhesive under shear loading was obtained experimentally by carrying out V-notched beam tests under four-point asymmetric loading following ASTM D5379 as shown in Figure 8 and Figure 9. The reason for selecting this test method is that a uniform shear load could easily be applied to the coupon regardless of the type of material tested. The average dimensions of test coupons were 3.0-inch (76 mm) long, 0.45-inch (11.4 mm) wide, and 0.08-inch (2 mm) thick. Four 1.25-inch long and 0.125-inch thick aluminum tabs were bonded on both faces of each coupon away from the test region to stabilize the coupons as recommended in ASTM D5379. The shear stress-strain response of these coupons are shown in Figure 10. It is clear that the shear response was nonlinear.

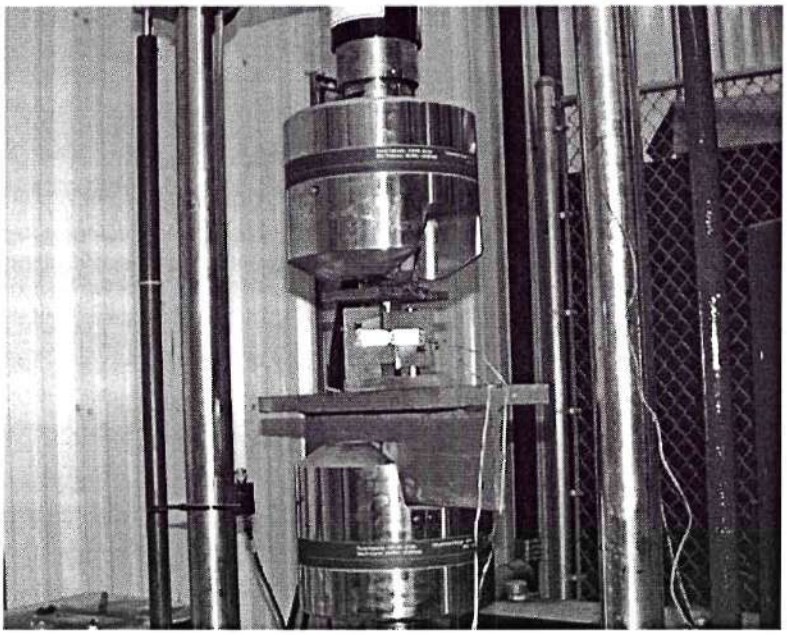

Figure 8. Shear test setup for Sikadur 30® epoxy coupons

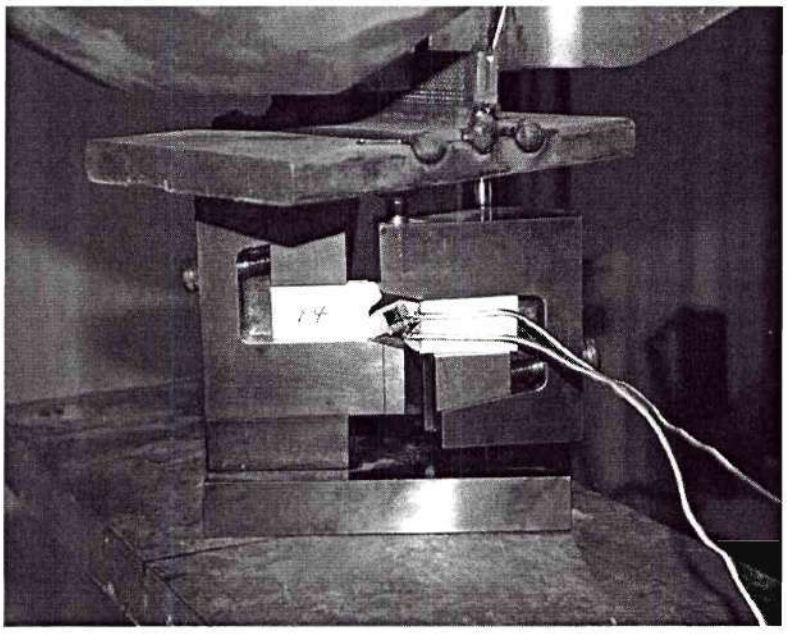

Figure 9. Iosipescu shear test fixture with a failed Sikadur 30® epoxy coupon (ASTM D5379)

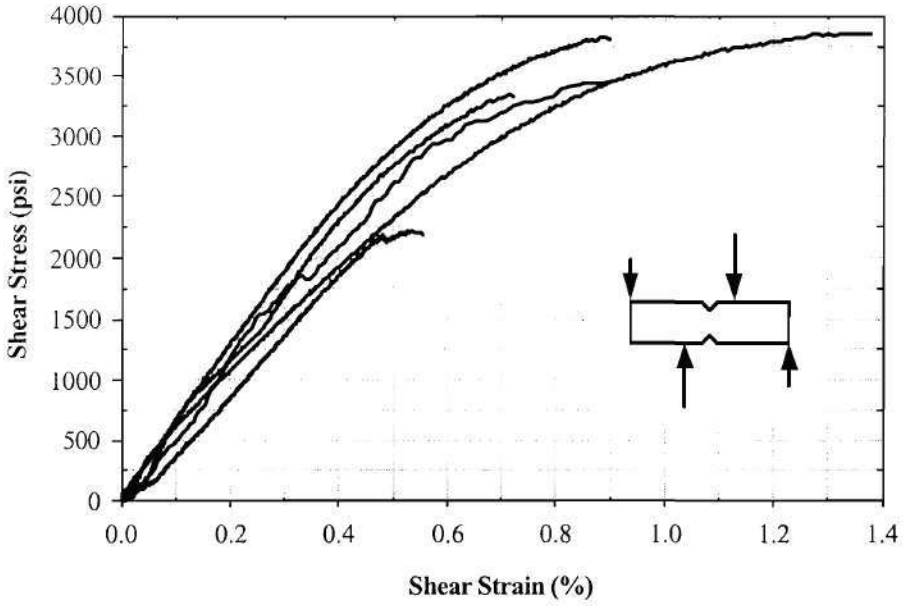

Figure 10. Shear stress-strain diagram of Sikadur 30® epoxy

CHAPTER III TESTS OF NON-REHABILITATED SLABS, RH-1 THROUGH RH-5

Specimens RH-1 through RH-5 first were loaded monotonically to a center deflection of 1.4-in. in order to significantly crack each specimen and to yield the tensile reinforcement. Figure 11 shows the load-deflection results for the five specimens. Table 2 lists the applied loads when the bottom and top reinforcing bars first yielded in tension and gives the load at the maximum 1.4-in. deflection (maximum crack width = 0.075 in.).

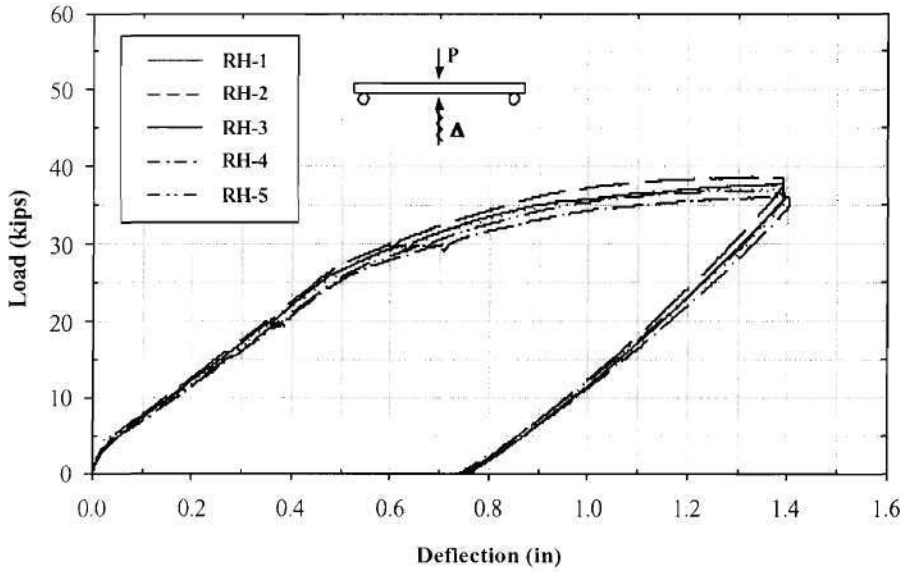

Figure 11. Load-deflection curves for non-rehabilitated slabs, RH-1 through RH-5

Table 2. Applied loads at different stages of tests

Specimen	Load at Yielding of Bottom Steel Layer (kips)	Load at Yielding of Top Steel Layer (kips)	Load at Deflection of 1.4 inch (kips)
RH-1	21.2	34.7	37.8
RH-2	22.8	36.1	38.7
RH-3	21.5	35.3	37.1
RH-4	Not measured	Not measured	36.1
RH-5	Not measured	Not measured	36.9

For specimen RH-1, the load reached a maximum value of 37.8 kips. The midspan load-deflection curves of the three potentiometers are shown in Figure12.

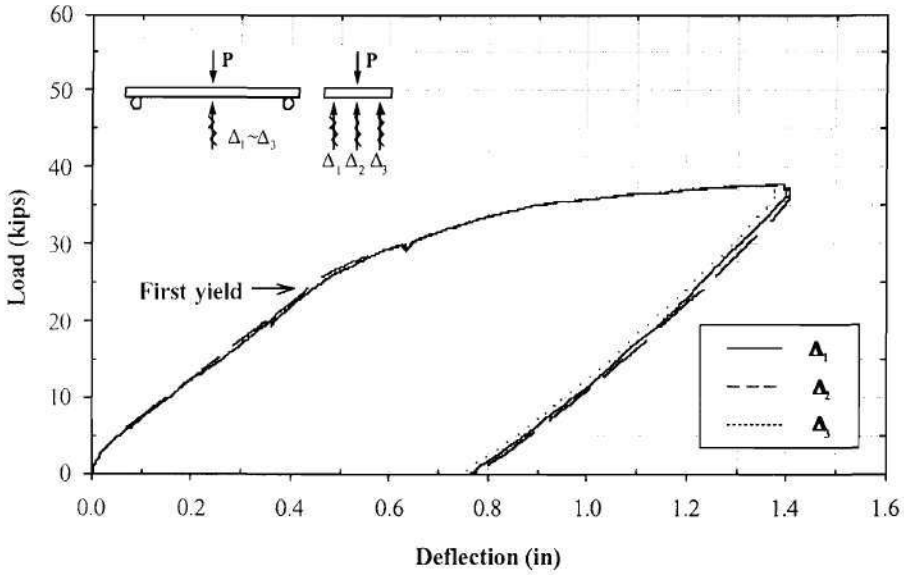

Figure 12. RH-1 load-deflection curves for non-rehabilitated test

The loads needed to yield the top and bottom layers of steel were calculated from the load-strain diagrams using the average steel yield strain obtained from material tests and then averaging the loads corresponding to the yield strain of each reinforcing bar.

When each specimen was unloaded, the cracks on the concrete tension face were measured to indicate the extent of plastic deformation. At mid-span, a crack of 0.075 inches in width was observed. Parallel cracks from mid-span towards the supports were measured to be 0.05, 0.025, and 0.007 inches in width.

Based on the measured strains from the top and bottom reinforcing bars, the theoretical moments (M_{calc}) applied to the specimens RH-1, RH-2, and RH-3 were calculated as given in Table 3. The average measured strain values were used to find the stress in the reinforcement at three different load levels: at 15 kips, at the load when first yielding of bottom bars occurred, and at 25 kips. The stress values were used to calculate the total tension force. The tension force was

equated to the compression in the concrete; the Todeschini parabolic stress block (MacGregor, 1997) was used to model the concrete compression and to compute the position of the neutral axis and resulting internal moment (M_{calc}).

The experimental moment applied to the specimen (M_{exp}) was calculated as $M_{exp}=P_{exp}L/4$. In Table 3, the experimental moment is compared to the theoretical moment as the ratio M_{calc}/M_{exp}. In all cases the ratio is greater than one which showed that the use of the Todeschini stress relation was non-conservative.

Table 3. Comparison of experimental and calculated results

Specimen	Load (kips)	Average Strain		Average Stress		M_{calc} (k-in)	M_{exp} (k-in)	M_{calc}/M_{exp}
		Top Steel (με)	Bottom Steel (με)	Top Steel (ksi)	Bottom Steel (ksi)			
RH-1	15	572	1,833	16.2	51.8	465.7	359.8	1.29
	21.2	784	2,560	22.2	72.4	641.0	507.9	1.26
	25	936	3,536	26.5	72.6	663.0	599.7	1.11
RH-2	14.9	479	1,686	13.5	47.7	421.9	358.3	1.18
	22.8	701	2,566	19.8	72.6	630.5	547.9	1.15
	25	861	3,022	24.3	72.6	653.0	599.9	1.09
RH-3	15	506	1,757	14.3	49.7	440.4	359.1	1.23
	21.5	733	2,562	20.7	72.4	634.2	515.0	1.23
	25	860	3,319	24.3	72.6	652.8	599.1	1.09

Preparation of Concrete Surface, Adhesive, and CFRP Plate

The bottom surfaces of all reinforced concrete test specimens were ground to the aggregate level with a hand-held grinder. Residue resulting from the grinding process was removed with compressed air. The CFRP plates were cleaned with methyl-ethyl-ketone (MEK). This was followed by mixing and then applying 1.6 mm (1/16 inch) thick Sikadur 30® adhesive layer to the cleaned side of the carbon plates, which in turn were placed by hand on the concrete surface. A hard rubber roller was then used to press the composite plates until small amount of adhesive was forced out the sides of the plates. The rehabilitated slab specimens were left to cure at least 7 days prior to any testing.

CHAPTER IV TESTS OF REHABILITATED SLABS, RH-1R THROUGH RH-5R

Testing of the rehabilitated specimens was the same as that of the unreinforced specimens. The load was applied in a deflection control mode at a rate of 0.1 inches per minute. During each test, the load was stopped approximately 10 kips increments so that each specimen could be visually inspected for possible delamination of the composite. Further, the researchers listened to and noted the cracking and "popping" sounds during each test; these noises evidenced deterioration of the CFRP plate-to-concrete bond.

Specimen RH-1R

At a load of approximately 24 kips at which the average value of the recorded strains of the three CFRP plates (ε_{CFRP}) was 2,489 $\mu\varepsilon$ (ε_{CFRP1}=2,561 $\mu\varepsilon$, ε_{CFRP2}=2,386 $\mu\varepsilon$, ε_{CFRP3}=2,520 $\mu\varepsilon$), a soft cracking sound was heard. When the load reached a value of 49.5 kips with ε_{CFRP}=5,749 $\mu\varepsilon$, the cracking sounds were very frequent and loud. The maximum load was recorded at 51.1 kips with ε_{CFRP}=6,538 $\mu\varepsilon$, and failure of the three CFRP plates occurred in the form of peeling-off of the CFRP plates combined with interlaminar shear failure (with the CFRP plates) that was evident as intermittent thin layers of carbon fibers remained bonded to the concrete surface in the delaminated portion of each plate. The test was terminated and the specimen was unloaded. Figures 13 and 14 show the failure of the CFRP plates for specimen RH-1R.

Figure 15 shows specimen RH-1R as seen from side AB where the horizontal cracks at the top surface indicate crushing of the concrete in compression.

Figure 16 shows the load-deflection curve obtained for the rehabilitated test of specimen RH-1R.

Figure 17 presents the measured load-strain relationships of the CFRP plates. The CFRP strain at which failure occurred was 6,581 $\mu\varepsilon$ in the middle plate (ε_{CFRP2}). The strains in CFRP plates 1 and 3 were 6,522 $\mu\varepsilon$ and 6,537 $\mu\varepsilon$, respectively. The average failure strain of the CFRP plates was computed to be 6,546 $\mu\varepsilon$. The load-strain curves show a reduction in slope, a reduced stiffness around 4,500 $\mu\varepsilon$, a value somewhat less than when frequent cracking sounds were heard.

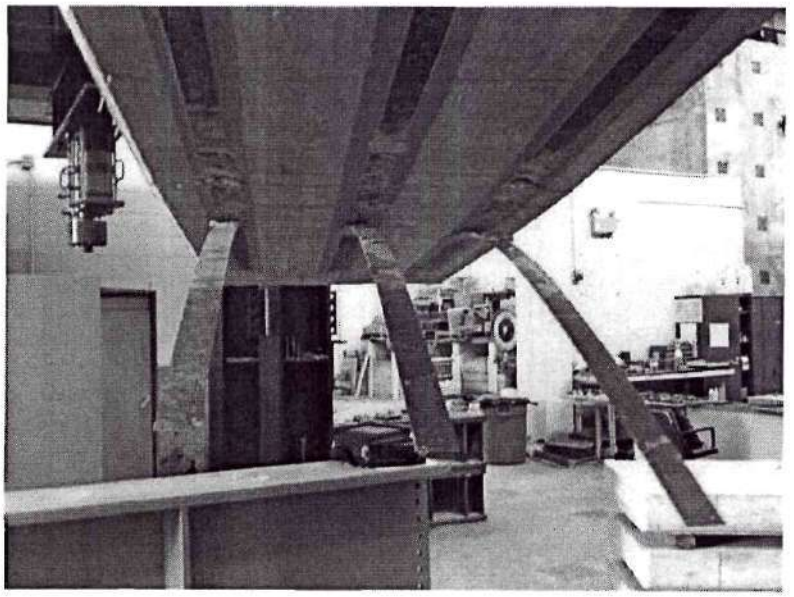

Figure 13. RH-1R failure mode of CFRP

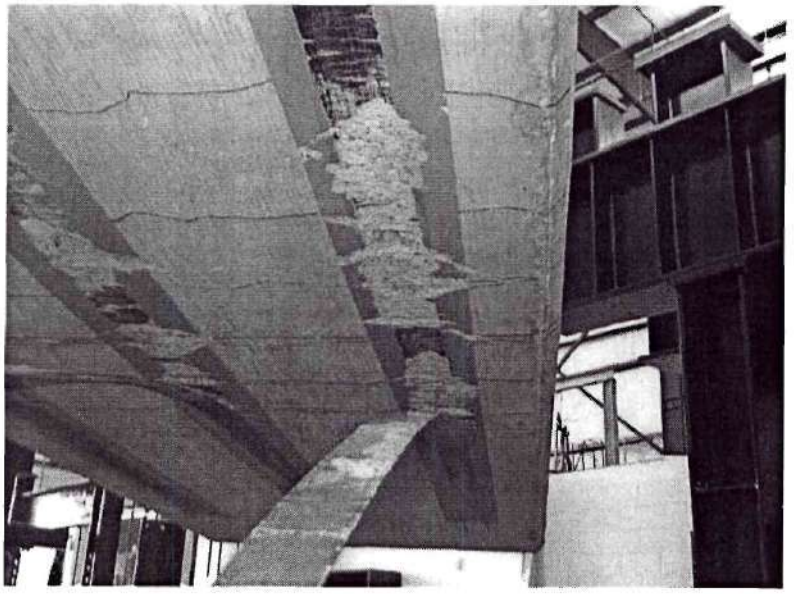

Figure 14. RH-1R failure mode of CFRP

Figure 18 shows the load-deflection curves for both the non-rehabilitated (RH-1) and rehabilitated (RH-1R) tests. The increase in the load-carrying capacity and stiffness of the slab

were computed to be 35.3 % and 35.6 %, respectively.

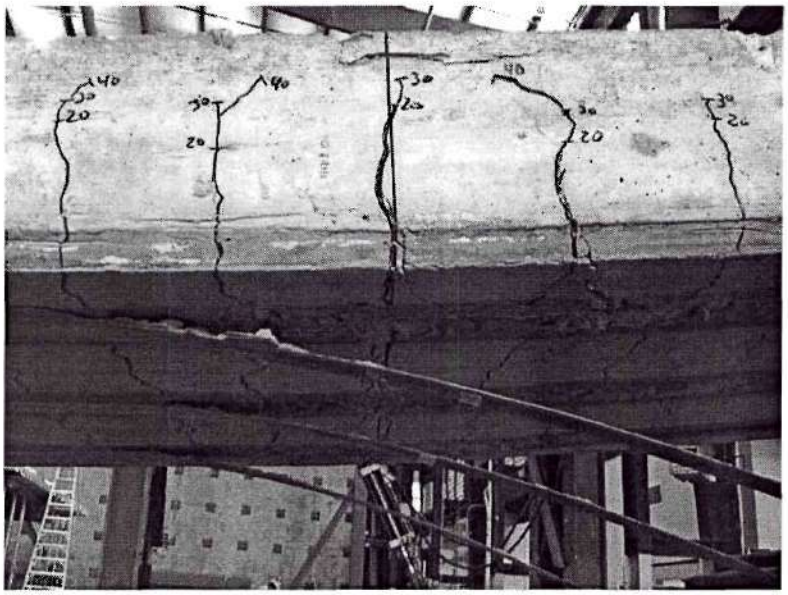

Figure 15. RH-1R crushing of the concrete from side AB

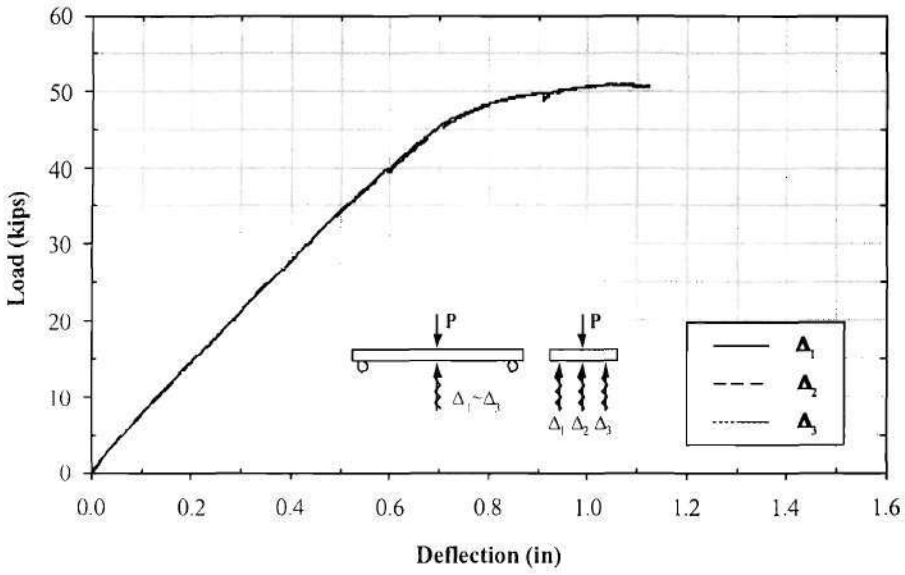

Figure 16. RH-1R load-deflection curves for rehabilitated test

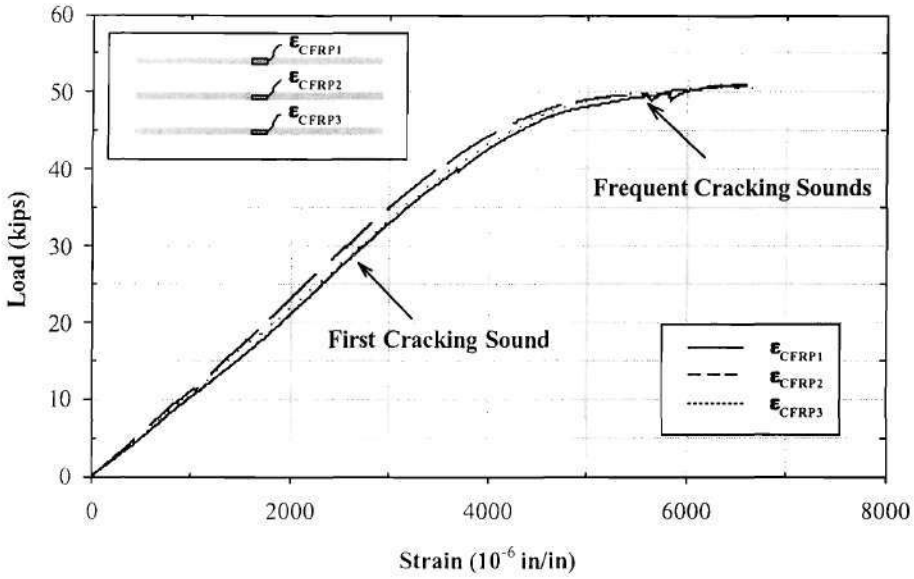

Figure 17. RH-1R load-CFRP strain for rehabilitated test

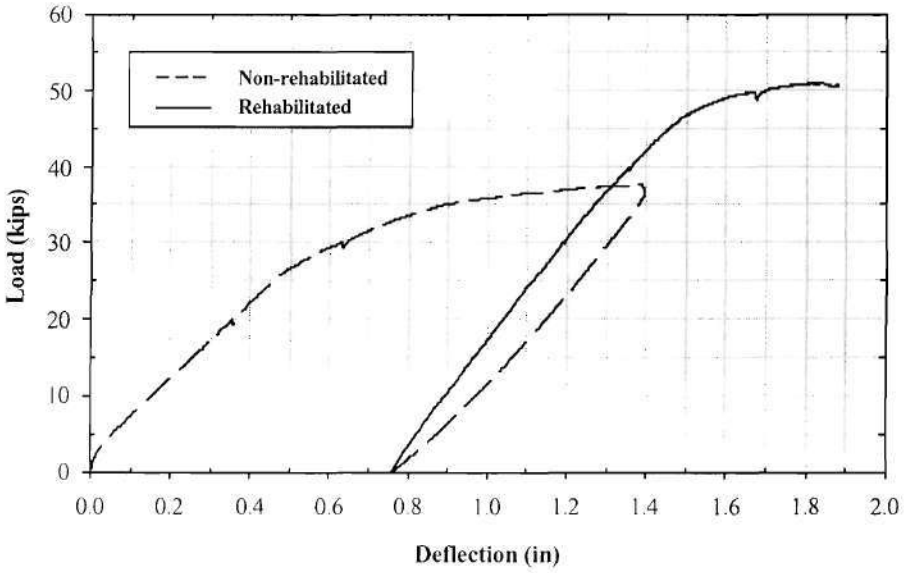

Figure 18. RH-1 load-deflection curves for non-rehabilitated and rehabilitated tests

Specimen RH-2R

At a load of approximately 37 kips at which ε_{CFRP}=3,772 με (ε_{CFRP1}=3,637 με, ε_{CFRP2}=3,995 με, ε_{CFRP3}=3,684 με), a soft cracking sound was heard. More frequent and louder cracking sounds were heard at a load of 47 kips with ε_{CFRP}=5,086 με. The maximum load obtained in the rehabilitated test of specimen RH-2R was recorded at 50.0 kips with ε_{CFRP}=6,320 με. The failure mode observed was very similar to that of specimen RH-1R with CFRP plate 2 delaminating first, followed by the delamination of plate 3 and plate 1. The test was then terminated and the load released gradually.

At failure, plate 2 strain (ε_{CFRP2}) was 6,251 με with ε_{CFRP1} and ε_{CFRP3} being 6,367 με and 6,575 με, respectively. Figure 19 shows the load-deflection curves for the original (RH-2) and for the rehabilitated (RH-2R) bridge deck specimen. The increase in the strength and stiffness after rehabilitation were 29.0 % and 41.2 %, respectively.

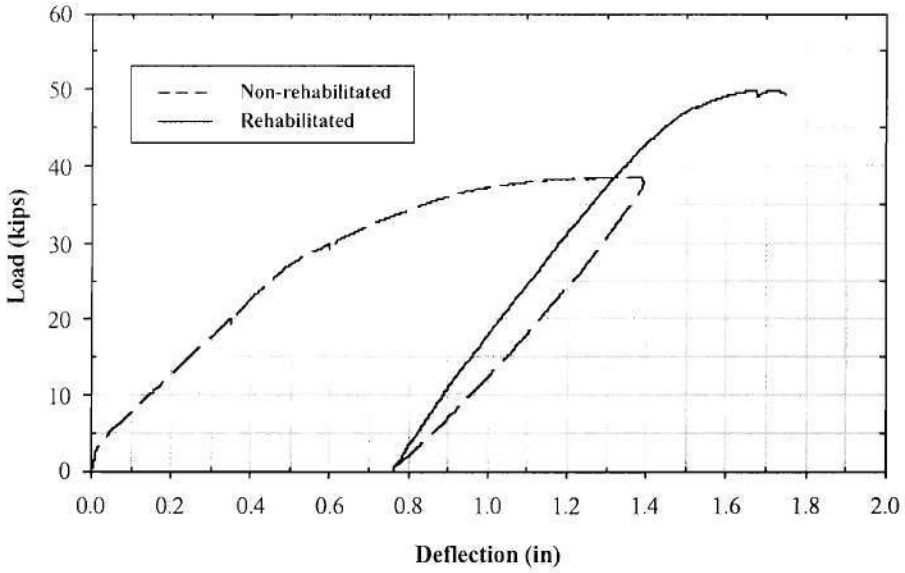

Figure 19. RH-2 load-deflection curves for non-rehabilitated and rehabilitated tests

The load-strain relationships for each CFRP plate of specimen RH-2R are shown in Figure 20. The 5,000 με location where the load-strain curves "yield" and show marked decrease in

stiffness corresponds to the occurrence of frequent cracking. The initiation of the non-linear load-strain response corresponds to the initiation of cracking sounds.

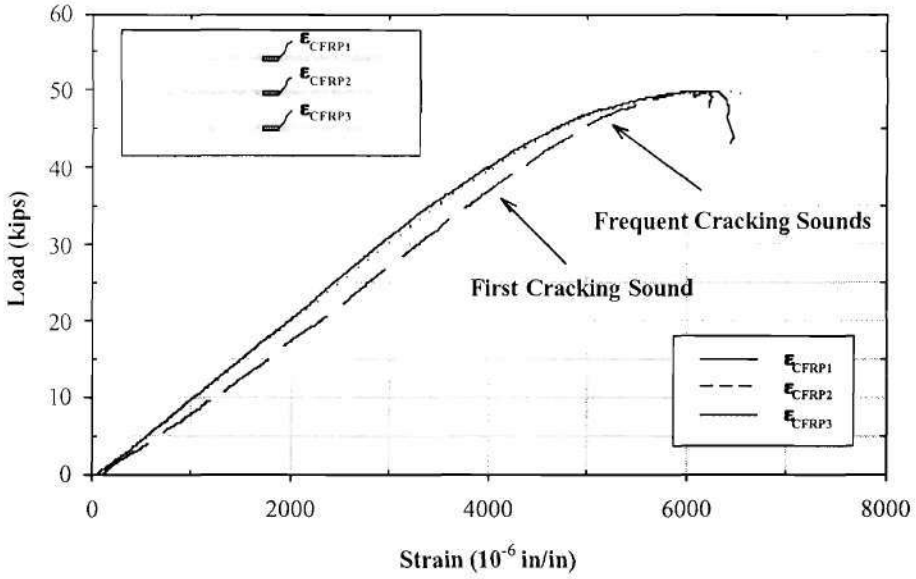

Figure 20. RH-2R load-CFRP strain for rehabilitated test

Specimen RH-3R

For specimen RH-3R the first cracking sound was heard when the load reached 34 kips with ε_{CFRP}=3,454 με (ε_{CFRP1}=3,086 με, ε_{CFRP2}=3,688 με, ε_{CFRP3}=3,586 με). The frequency of the cracking sounds increased as the load reached 46.8 kips with ε_{CFRP}=5,521 με. At a load of 47.3 kips delamination of the three CFRP plates occurred. The failure mode was similar to those observed in specimens RH-2R and RH-3R.

The strains at failure in CFRP plates 1, 2, and 3 were 5,684 με, 6,116 με, and 6,395 με, respectively. Figure 21 shows the load-deflection curves for the original (RH-3) and for the rehabilitated (RH-3R) bridge deck. The increase in the strength and stiffness after rehabilitation were 27.3 % and 19.2 %, respectively. Figure 22 presents the load-strain response for the CFRP plates of specimen RH-3R. Again, the initiation of non-linear response corresponded to the first cracking sounds, and significant reduction in stiffness corresponds to frequent cracking.

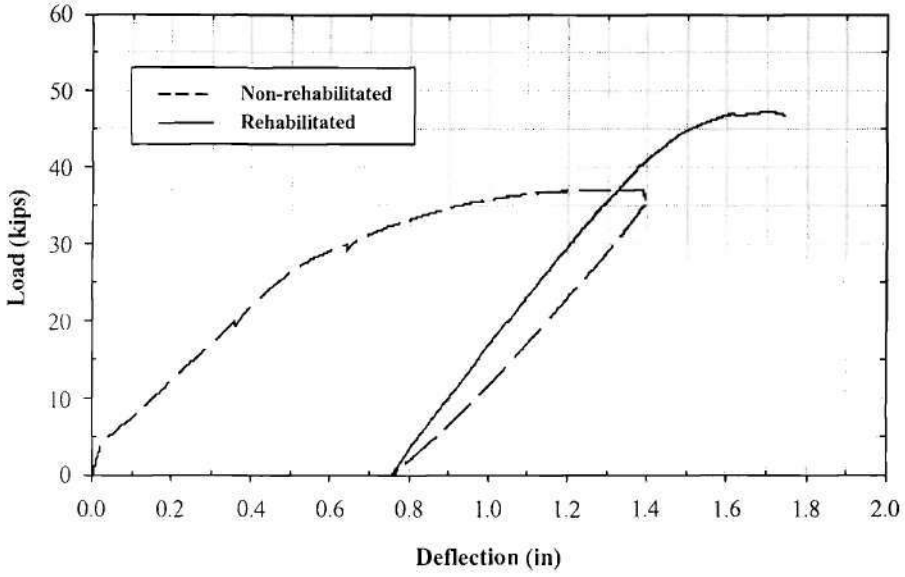

Figure 21. RH-3 load-deflection curves for non-rehabilitated and rehabilitated tests

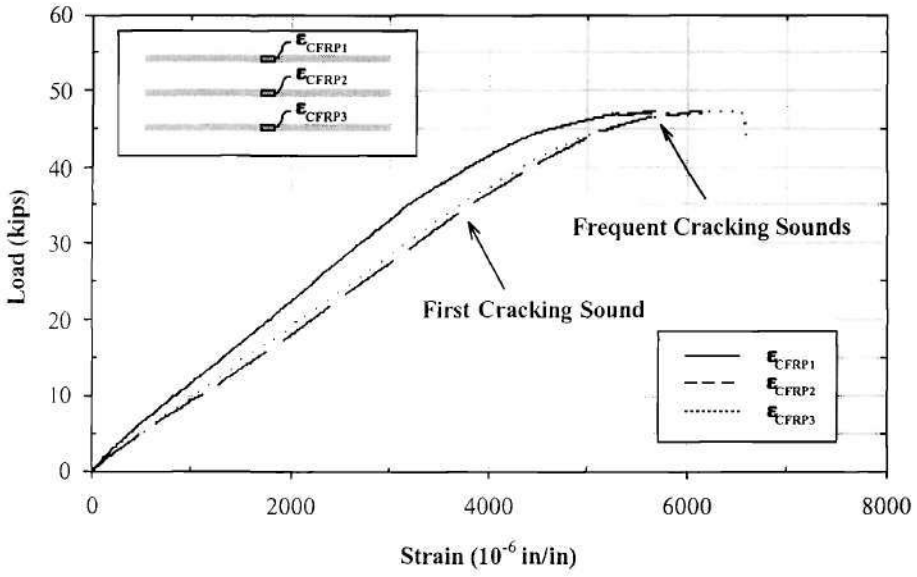

Figure 22. RH-3R load-CFRP strain for rehabilitated test

Specimen RH-4R

The first cracking sound for specimen RH-4R was heard at a load of 35 kips with ε_{CFRP}=3,388 με (ε_{CFRP1}=3,318 με, ε_{CFRP2}=3,344 με, ε_{CFRP3}=3,489 με, ε_{CFRP4}=3,401 με). The frequency of the cracking sounds increased as the load reached 47.7 kips with ε_{CFRP}=5,211 με. The specimen was able to carry a maximum load of 48.7 kips, and failure occurred in a manner similar to those found in the previous specimens. Figure23 shows the failure of specimen RH-4R.

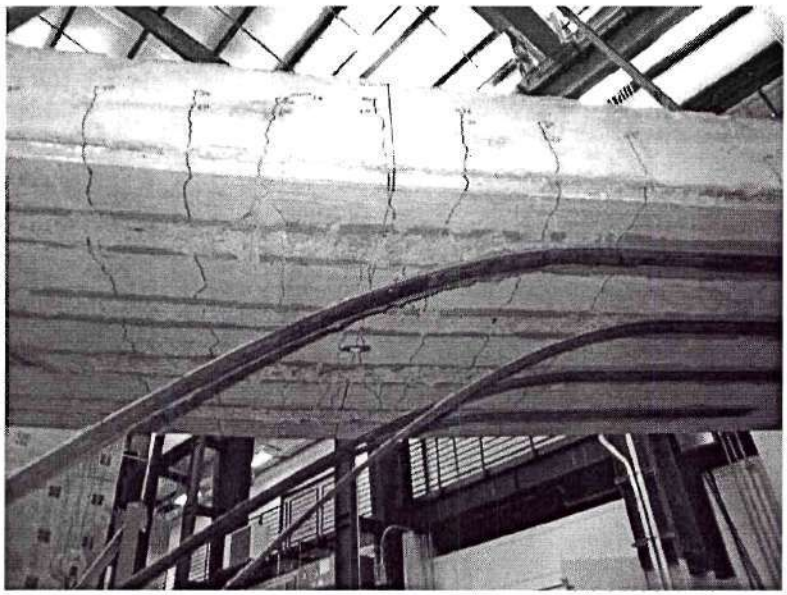

Figure 23. RH-4R failure mode of CFRP

Figure 24 shows the load-deflection curves obtained for the original (RH-4) and rehabilitated (RH-4R) bridge deck. Figure25 shows the load-strain response for the CFRP plates of specimen RH-4R.

At failure, the strains in plates 1, 2, 3, and 4 were 5,547 με, 5,594 με and 5,712 με, 5,570 με, respectively; the average failure strain was 5,606 με. As in the specimens with three plates, the initiation of non-linear load-strain response corresponds to initiation of cracking sounds.

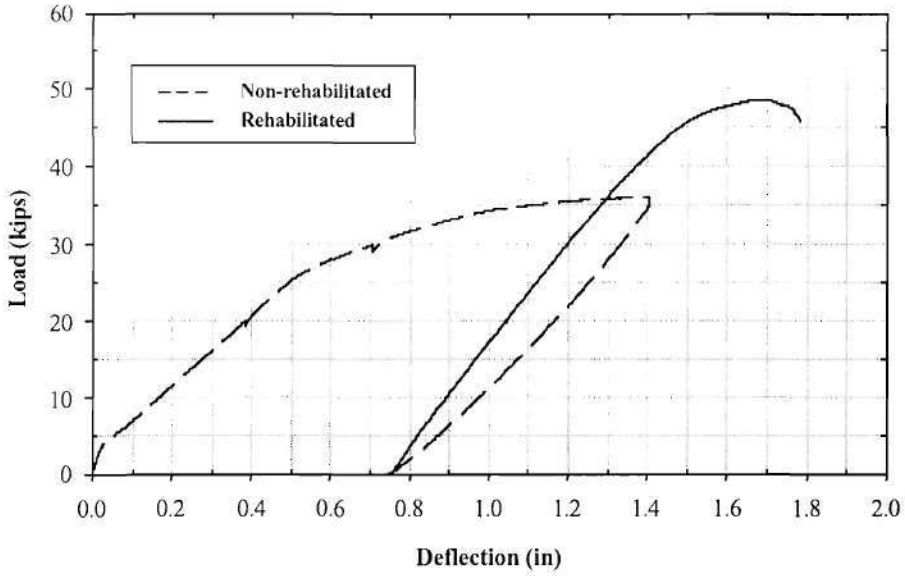

Figure 24. RH-4 load-deflection curves for non-rehabilitated and rehabilitated tests

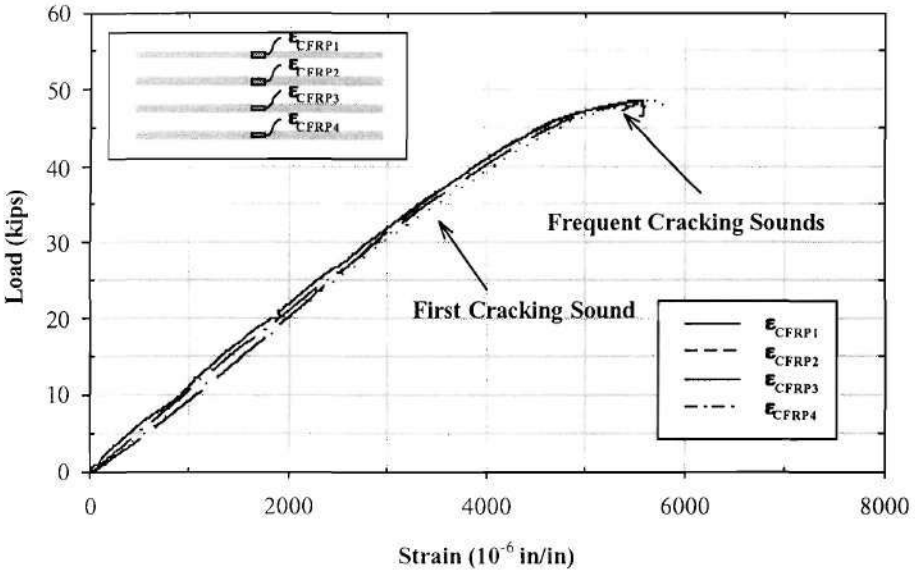

Figure 25. RH-4R load-CFRP strain for rehabilitated test

Specimen RH-5R

For specimen RH-5R the first soft cracking sound was heard at a load of 29 kips with ε_{CFRP}=2,717 με (ε_{CFRP1}=2,899 με, ε_{CFRP2}=2,730 με, ε_{CFRP3}=2,423 με, ε_{CFRP4}=2,717 με). Frequent and louder cracking sounds were heard when the load reached 49.5 kips with ε_{CFRP}=5,062 με. Delamination of the CFRP plates occurred at 50.6 kips.

The strains at failure in plates 1, 2, 3, and 4 were 5,910 με, 5,225 με, 5,121 με, and 5,149 με, respectively; the average strain was 5,351 με. Figure 26 shows the load- deflection curves for the non-rehabilitated (RH-5) and for the rehabilitated (RH-5R) bridge decks. Figure 27 presents the load-strain response for the CFRP plates of specimen RH-5R. Plates 2 and 4 showed a stiffening response at 2,500 με and 1,700 με, respectively. Frequent cracking occurred after the load-strain response showed significant softening.

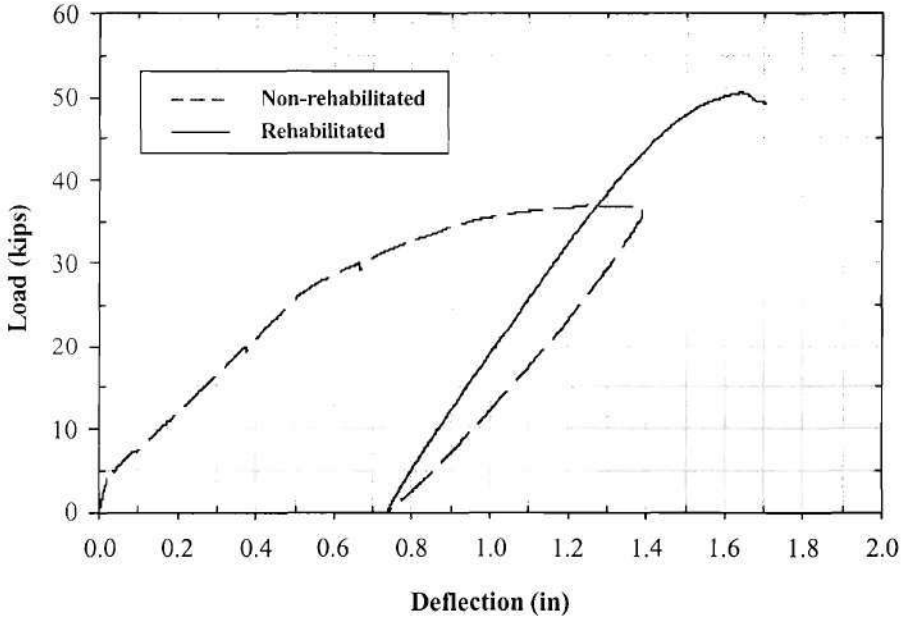

Figure 26. RH-5 load-deflection curves for non-rehabilitated and rehabilitated tests

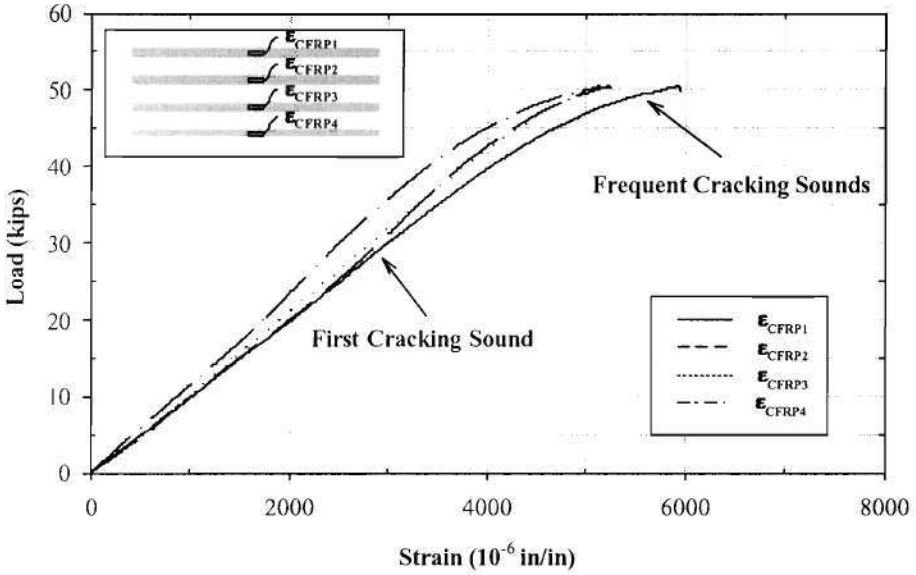

Figure 27. RH-5R load-CFRP strain for rehabilitated test

Comparison of Test Results for Rehabilitated Specimens

The results of the five rehabilitated specimens were compared by first reviewing the load-deflection responses shown in Figure 28 and by listing the maximum loads found in the original and in the rehabilitated specimens in Table 4. The overall response of the five specimens was similar. Of particular note was that the maximum strength of the specimens with 4 plates was about the same as the maximum strength of those rehabilitated with 3 plates. The average maximum load of specimens RH-4R and RH-5R was 49.6 kips while the average maximum load of specimens RH-1R, 2R, and 3R was 49.5 kips. That these two groups showed the same strength resulted because the failure of each specimen was governed by delamination of the CFRP plates. On average, the rehabilitated specimens were 33 percent stronger than the original, non-rehabilitated bridge deck specimens.

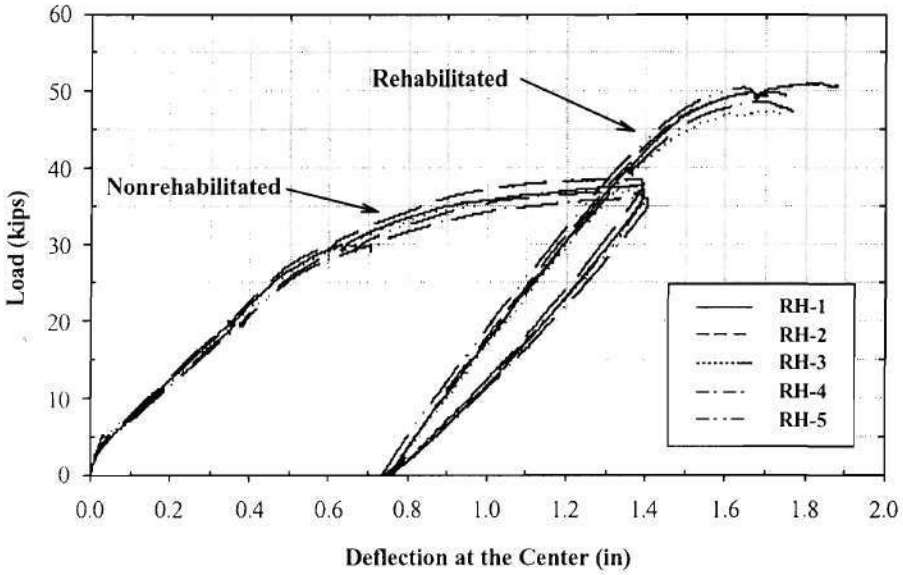

Figure 28. Load-deflection curves for non-rehabilitated and rehabilitated specimens

Table 4. Group RH load results

Specimen	Max. Load of Non-Rehabilitated Specimen (kips)	Max. Load of Rehabilitated Specimen (P_{exp}, kips)	Increase of Max. Load by Rehabilitation (%)	Calculated Max. Load After Rehabilitation (P_{calc}, kips)	P_{exp}/P_{calc}
RH-1	37.8	51.1	35	42.4	1.20
RH-2	38.7	50.0	29	42.1	1.19
RH-3	37.1	47.3	27	41.6	1.14
Average RH-1 ~ RH-3	37.9	49.5	31	42.0	1.18
RH-4	36.1	48.7	35	43.3	1.13
RH-5	36.9	50.6	37	42.7	1.18
Average RH-4, RH-5	36.5	49.6	36	43.0	1.15
Average All Specimens	37.3	49.5	33	42.4	1.17

The rehabilitated specimens were in general stiffer than the non-rehabilitated slab specimens. As listed in Table 5, the elastic, flexural stiffness of each specimen was calculated as the load divided by the center deflection of 0.4 inches ($48\ D/L^3$). These results show that epoxy

bonding CFRP plates to the tension face of slabs not only increases flexural strength but also increases post-crack flexural stiffness.

Table 5. Stiffness comparison for Group RH specimens

Specimen	Non-Rehabilitated (kips/in)	Rehabilitated (kips/in)	Increase of Stiffness (%)
RH-1	55.4	69.5	25
RH-2	56.4	72.3	28
RH-3	54.5	67.3	24
Average RH-1 ~ RH-3	55.4	69.7	26
RH-4	51.6	68.4	32
RH-5	52.5	71.0	35
Average RH-4, RH-5	52.1	69.7	34
Average	54.1	69.7	29

An important goal of this research was to investigate the failure mode of CFRP reinforced slabs and to determine critical design parameters. One such parameter was the maximum strain in the CFRP plates. Table 6 lists the maximum strains in each plate for each specimen, gives the average maximum strain, and shows the coefficient of variation of those strains. The average failure strain for specimens with 3 plates was 6,336 με while the average for the specimens with 4 plates was 5,479 με.

Table 6. Strains at failure in Sika Carbodur® CFRP plates

Specimen	FS1 (με)	FS2 (με)	FS3 (με)	FS4 (με)	Average (με)	C.O.V. (%)
RH-1	6,522	6,581	6,537	N/A	6,546	0.5
RH-2	6,367	6,251	6,575	N/A	6,398	2.6
RH-3	5,684	6,116	6,395	N/A	6,065	5.9
RH-4	5,547	5,594	5,712	5,570	5,606	1.3
RH-5	5,910	5,225	5,149	5,121	5,351	7.0

The approximate loads and average CFRP strain values were noted at the time the carbon fibers emitted cracking sounds. It was observed that the CFRP strain at which cracking

sounds were heard was proportional to the CFRP strain at failure. For the Sika Carbodur® system, the acoustic emissions were first heard when the average CFRP strain(ε_{CFRP}) reached values ranging from 33% to 60% of the CFRP plate strain when failure occurred. Frequent and louder sounds were heard at between 79% and 95% of strains at failure. Table 7 provides a summary of these results.

Because the cracking sounds were a precursor to delamination failure, it seems reasonable to use the total average strain of CFRP plates when first cracking sound was heard to limit the maximum strain in the CFRP plates. Therefore, a practical limitation for service load may be taken as 3,151 με, or approximately 3,000 με. The frequent cracking sounds for specimens RH-1R through RH-5R occurred at an average strain of 89% of the strain at failure, or at an average strain of 5,303 με. It may be postulated that this value represents an effective ultimate strain.

Table 7. Group RH correlation between perceived noises and CFRP plate failure strain

Specimen		First Cracking	Frequent Cracking	At Failure
RH-1R	Load (P, kips)	28	49.5	51.0
	Average Strain of CFRP (ε_{CFRP}, με)	2,489	5,749	6,546
	% of ε_{CFRP} at Failure	38%	88%	100%
RH-2R	Load (P, kips)	37	47	49.1
	Average Strain of CFRP (ε_{CFRP}, με)	3,772	5,086	6,398
	% of ε_{CFRP} at Failure	59%	79%	100%
RH-3R	Load (P, kips)	34	46.8	47.3
	Average Strain of CFRP (ε_{CFRP}, με)	3,454	5,521	6,065
	% of ε_{CFRP} at Failure	57%	91%	100%
RH-4R	Load (P, kips)	35	47.7	48.6
	Average Strain of CFRP (ε_{CFRP}, με)	3,388	5,211	5,606
	% of ε_{CFRP} at Failure	60%	93%	100%
RH-5R	Load (P, kips)	29	49.5	50.6
	Average Strain of CFRP (ε_{CFRP}, με)	2,717	5,062	5,351
	% of ε_{CFRP} at Failure	51%	95%	100%
All Specimens	Average Load (P, kips)	32.6	48.1	49.3
	Average Strain of CFRP (ε_{CFRP}, με)	3,151	5,303	5,933
	% of ε_{CFRP} at Failure	53%	89%	100%

CHAPTER V TESTS OF STRENGTHENED SLABS, ST-1 THROUGH ST-6

Specimen ST-1

Figure 29 shows the load-deflection response of ST-1; all deflection gages were consistent. Concrete cracked at about 8 kips and the bottom steel yielded at about 35 kips. The ultimate load was 49.6 kips at which the CFRP plates delaminated. The top layer of steel did not yield. Figure 30 shows the load-CFRP strain results. The CFRP strains were consistent with an ultimate, average strain of 6,116 με. The delamination cracking sounds started at a CFRP strain of 4,153 ìå, and they became frequent at a strain of 5,302 με.

Figure 31 shows the strain profiles through the depth of the cross section for four load cases that represent the loads in the linear region (P=20 kips), at the first cracking of CFRP plate, at the frequent cracking of CFRP plate, and at the ultimate, respectively. The theoretical strain profile based on a Todeschini stress block is presented as solid lines with strain values at the top surface and CFRP in parentheses in Figure 31, while the average measured strains at top steel layer, bottom steel layer, and CFRP are presented as dots.

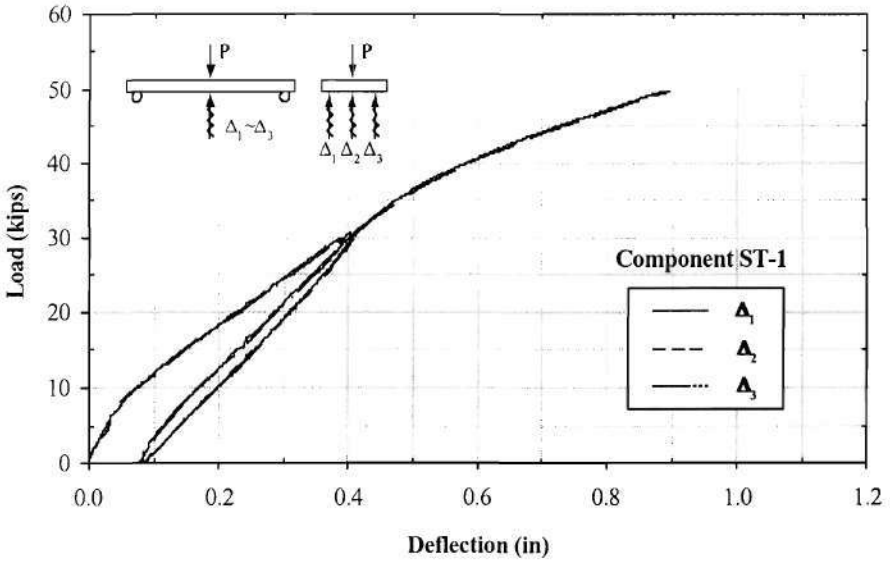

Figure 29. ST-1 load-deflection curves

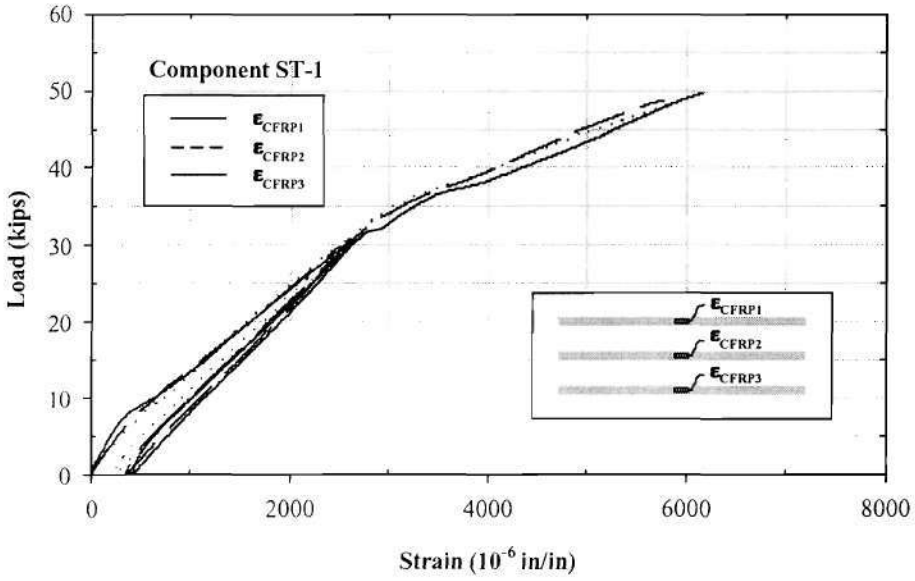

Figure 30. ST-1 load-CFRP strain curves

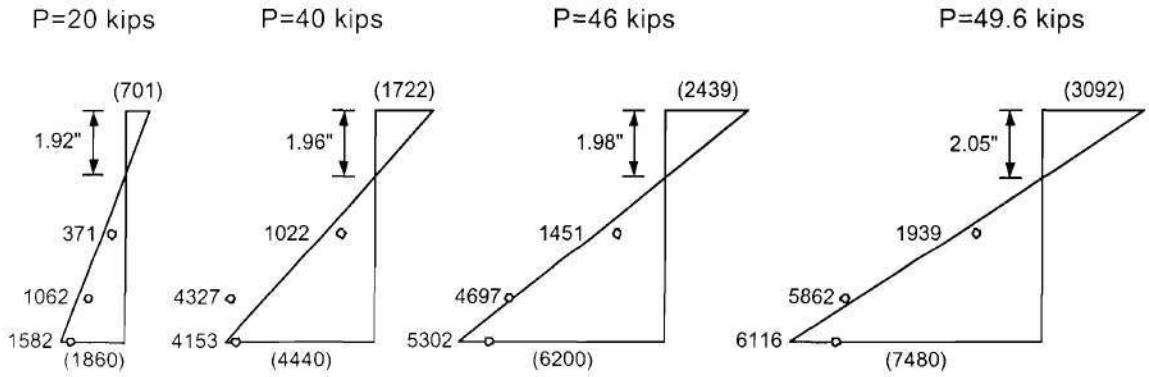

Figure 31. ST-1 strain profiles

Specimen ST-2

Figure 32 shows the load-deflection response of ST-2; all deflection gages were consistent. Concrete cracked at about 5 kips and the bottom steel yielded at about 33 kips. The ultimate load was 44.7 kips at which the CFRP plates delaminated. The top layer of steel did not

yield. Figure 33 shows the load-CFRP strain results. The CFRP stains were consistent with an ultimate, average strain of 5,810 με. The delamination cracking sounds started at a CFRP strain of 4,204 με, and they became frequent at a strain of 4,994 με. Figure 34 shows the strain profile through the depth of the cross section for four load cases.

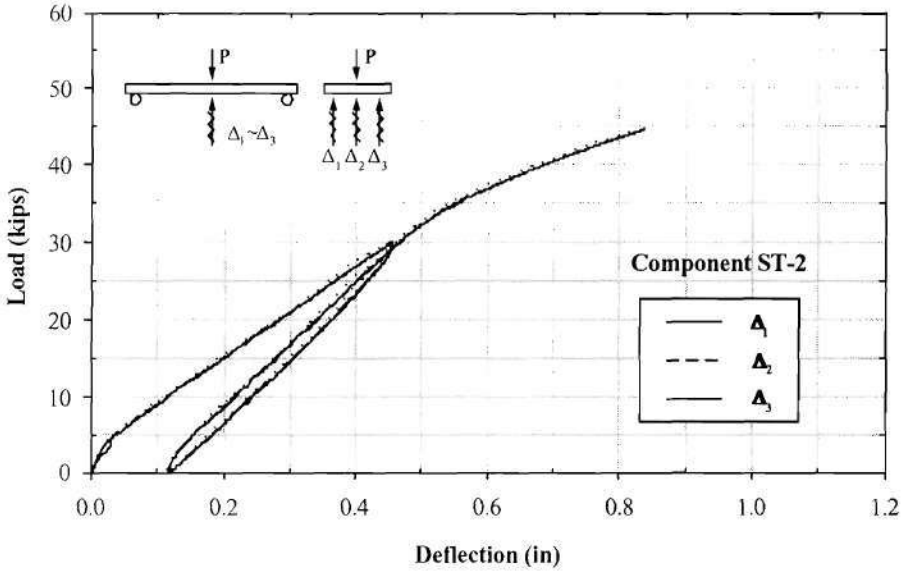

Figure 32. ST-2 load-deflection curves

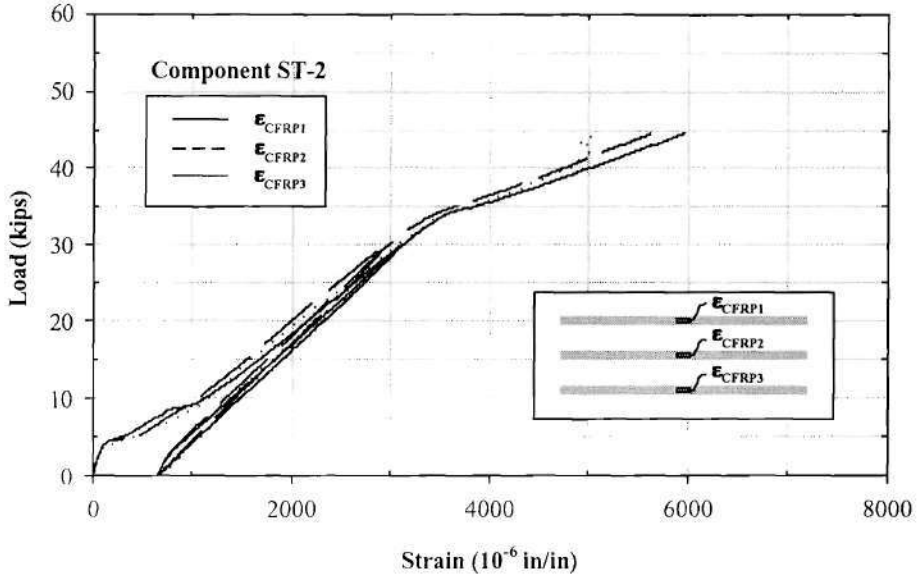

Figure 33. ST-2 load-CFRP strain curves

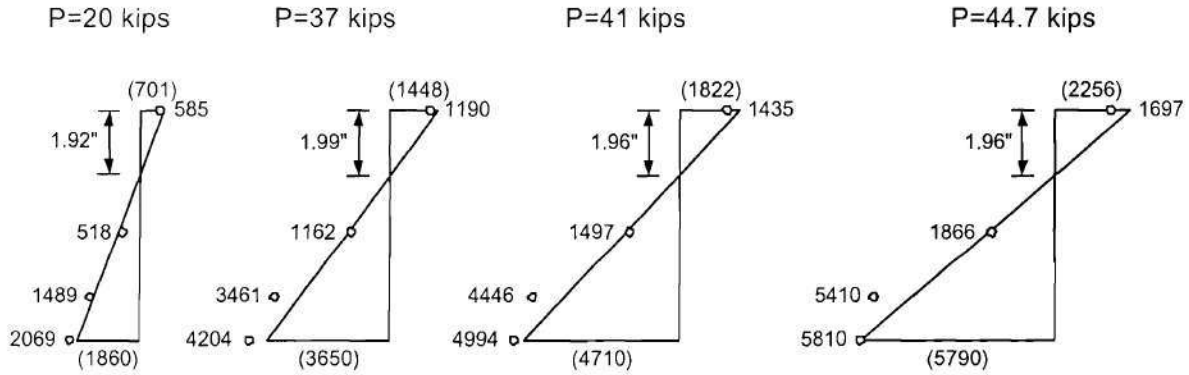

Figure 34. ST-2 strain profiles

Specimen ST-3

Figure 35 shows the load-deflection response of ST-3; all deflection gages were consistent. Concrete cracked at about 5 kips and the bottom steel yielded at about 36 kips. The ultimate load was 50.0 kips at which the CFRP plates delaminated. Figure 36 shows the load-CFRP

strain results. The CFRP stains were consistent with an ultimate, average strain of 6,713 με. The delamination cracking sounds started at a CFRP strain of 4,968 με, and they became frequent at a strain of 5,662 με. Figure 37 shows the strain profile through the depth of the cross section for four load cases.

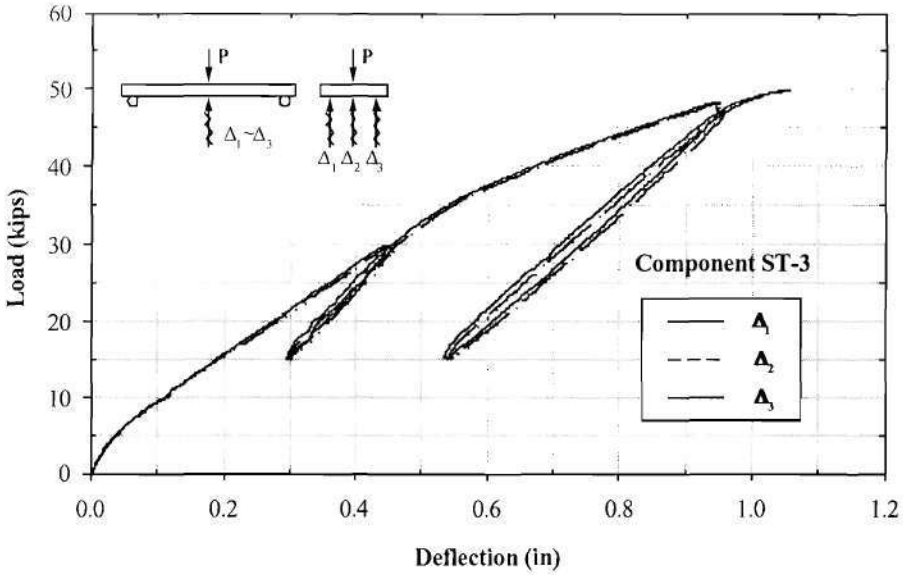

Figure 35. ST-3 load-deflection curves

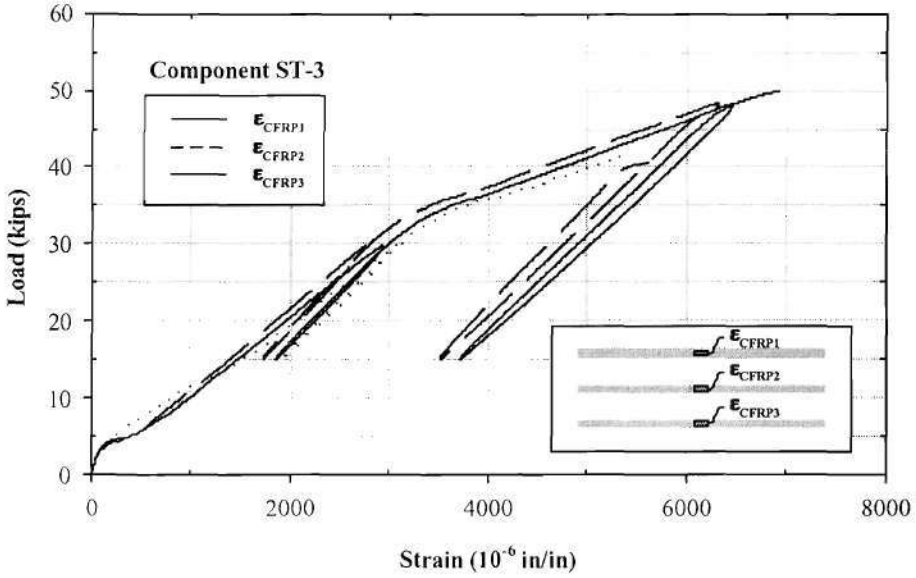

Figure 36. ST-3 load-CFRP strain curves

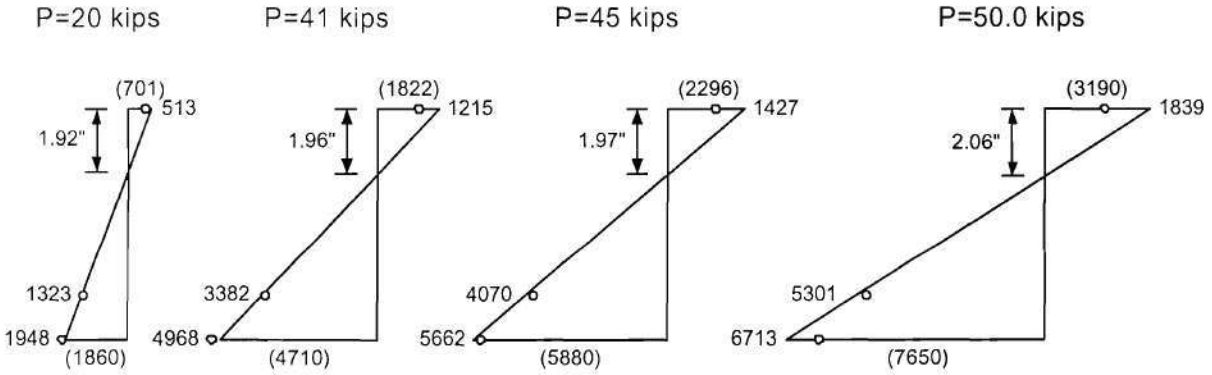

Figure 37. ST-3 strain profiles

Specimen ST-4

Figure 38 shows the load-deflection response of ST-4; all deflection gages were consistent. Concrete cracked at about 8 kips and the bottom steel yielded at about 24 kips. The load-deflection curve changes slop at about 18 kips indicating yielding. The ultimate load was 49.6

kips at which the CFRP plates delaminated. The top layer of steel did not yield. Figure 39 shows the load-CFRP strain results. Since the strain gage on the CFRP2 plate did not function throughout the test, only two CFRP strain results were plotted. The average CFRP stain at the ultimate was 6,966 με. The delamination cracking sounds started at a CFRP strain of 4,600 με, and they became frequent at a strain of 6,050 με.

Figure 40 shows the strain profile through the depth of the cross section for four load cases. The strain shown is the strain parallel to the length of the specimen and is less than the strain parallel to the direction of the CFRP plates.

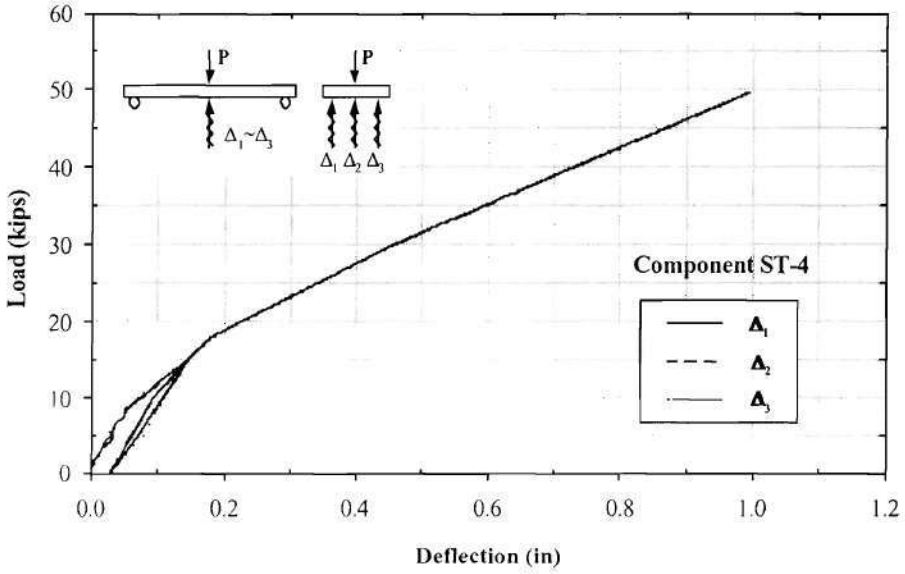

Figure 38. ST-4 load-deflection curves

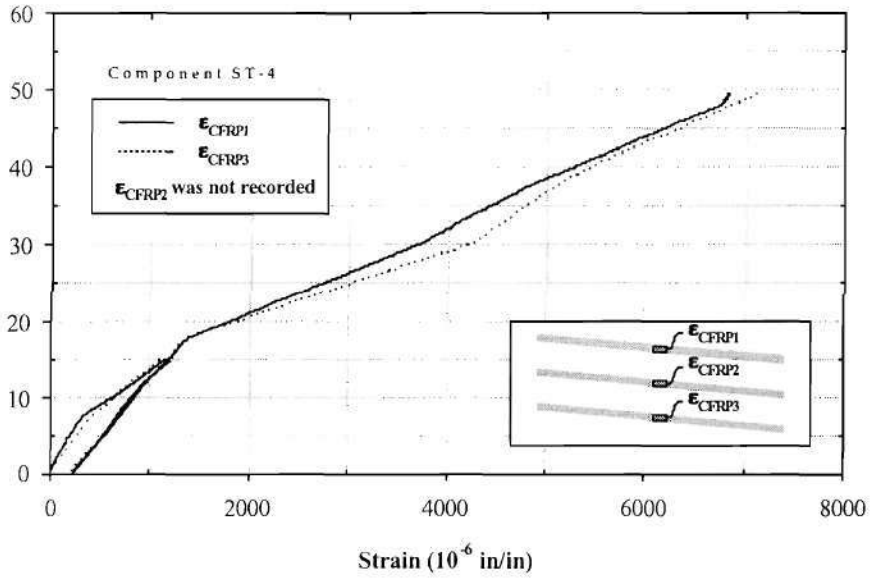

Figure 39. ST-4 load-CFRP strain curves

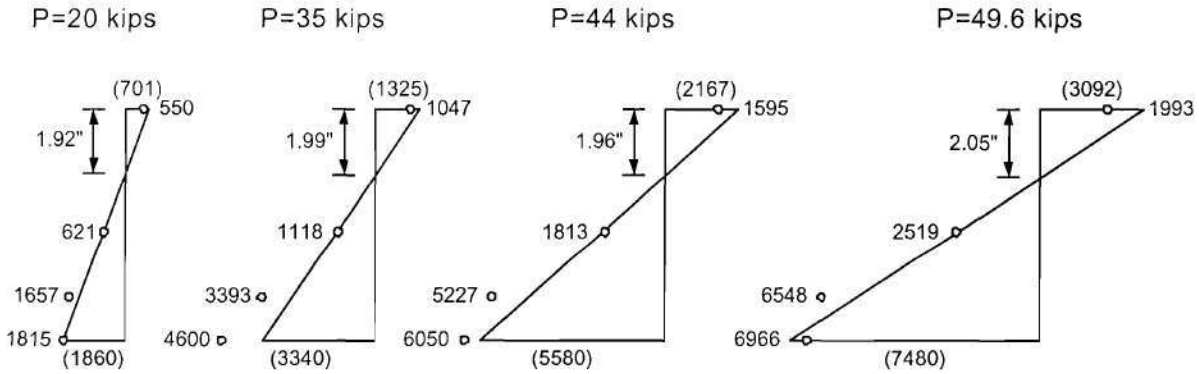

Figure 40. ST-4 strain profiles

Specimen ST-5

Figure 41 shows the load-deflection response of ST-5; all deflection gages were consistent. The change of slope in the load-deflection curve was at 31 kips, indicating yielding of the bottom steel layer. The ultimate load was 43.4 kips at which the CFRP plates delaminated. Fig-

ure 42 shows the load-CFRP strain results. The CFRP stains were consistent until the load reached about 40 kips, but all three strain rosettes were lost before the frequent cracking sounds were heard. The delamination cracking sounds started at an average CFRP strain of 5,118 με. The strain profile of this specimen is not presented since the strain gages on the top and bottom steel layers did not function throughout the test.

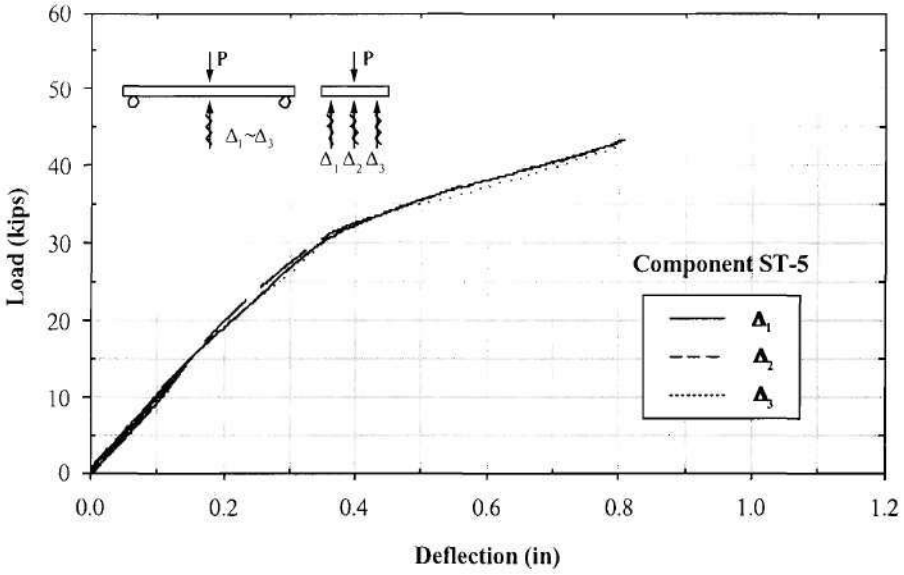

Figure 41. ST-5 load-deflection curves

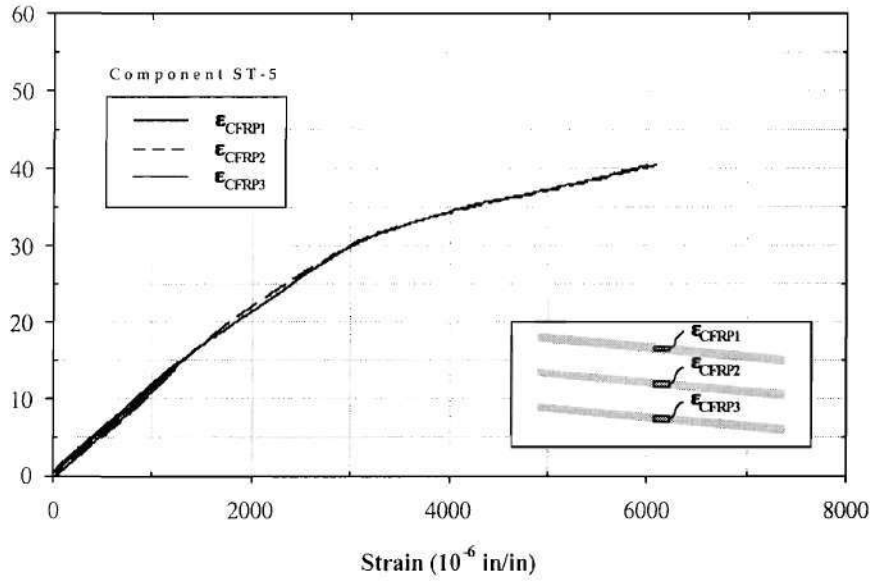

Figure 42. ST-5 load-CFRP strain curves

Specimen ST-6

The deflection gages did not operate correctly, so the load-deflection response of ST-6 is not presented. The bottom steel yielded at about 26 kips. The ultimate load was 44.7 kips at which the FRP plates delaminated. The top layer of steel did not yield. Figure 43 shows the load-CFRP strain results. Since the strain gage on the CFRP3 plate did not function throughout the test, only two CFRP strain results were plotted. The average CFRP stain at the ultimate was 6,962 με. The delamination cracking sounds started at a CFRP strain of 4,740 με, and they became frequent at a strain of 6,515 με.

Figure 44 shows the strain profile through the depth of the cross section for four load cases. The strain shown is the strain parallel to the length of the specimen and is less than the strain parallel to the direction of the CFRP plates.

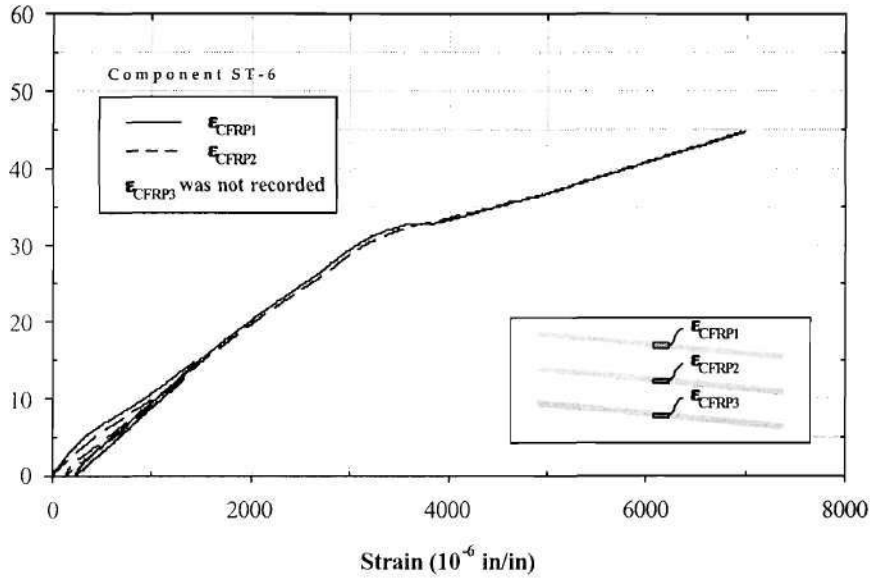

Figure 43. ST-6 load-CFRP strain curves

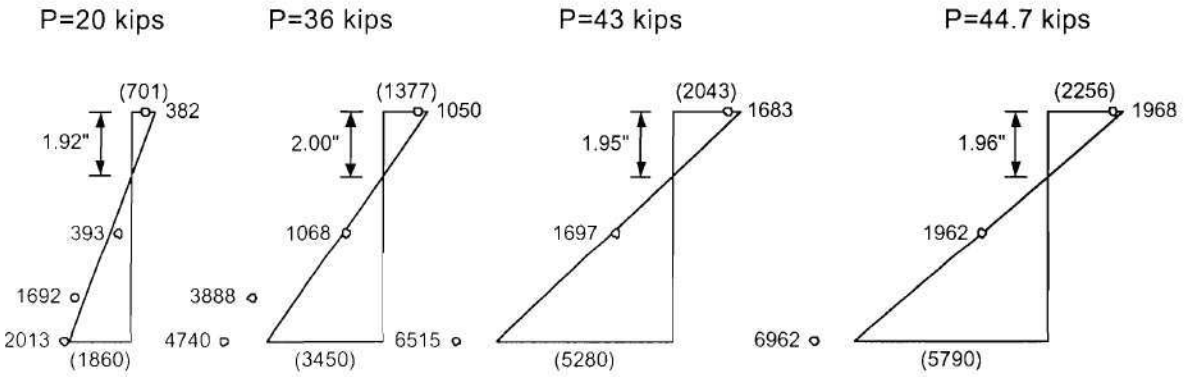

Figure 44. ST-6 strain profiles

Comparison between Specimens ST-1 through ST-3 and ST-4 through ST-6: Effect of Misalignment of CFRP plates

Tables 8 through 11 summarize the experimental data for test specimens ST-1 through ST-6. The average strength of the non-rehabilitated specimens RH-1 through RH-5 was 37.3

kips as given in Table 8. The average strength of ST-1 through ST-3 was 48.1 kips which was 29 percent greater than the non-rehabilitated specimen. The average strength of ST-4 through ST-6 was 45.9 kips which was 23 percent greater than the non-rehabilitated specimens. Overall, the addition of the three CFRP plates increased the strength of the bridge deck panels by about 26 percent.

Panels ST-4 through ST-6 with the CFRP plates misaligned by 5 degrees had an average ultimate strength less than 5 percent lower than the panels ST-1 through ST-3 which had aligned CFRP plates. Based upon the scatter of the data, the misalignment of the plates by 5 percent did not significantly decrease the ultimate strength of the rehabilitated bridge deck panels.

The average load at yield of panels ST-4 through ST-6 was 26 kips while that of ST-1 through ST-3 was 35 kips; the panels with the misaligned CFRP plates had an average yield load 26 percent less than the panels with the perfectly aligned plates. This lower average yield load indicates that the misalignment of the CFRP plates may affect the allowable service load of the strengthened panels more than misalignment affects the ultimate strength.

Table 8. Group ST load results

Specimen	Average Max. Load of Unstrengthened Specimens (kips)	Max. Load of Strengthened Specimen (P_{exp}, kips)	Increase of Max. Load by Strengthening (%)	Calculated Max. Load After Strengthening (P_{calc}, kips)	P_{exp}/P_{calc}
ST-1	37.3	49.6	33	44.5	1.11
ST-2		44.7	20	43.7	1.02
ST-3		50.0	34	46.2	1.08
Average ST-1 ~ ST-3		48.1	29	44.8	1.07
ST-4	37.3	49.6	33	46.8	1.06
ST-5		43.4	16	N.A.	N.A.
ST-6		44.7	20	46.8	0.96
Average ST-4 ~ ST-6		45.9	23	46.8	1.01
Average All Specimens	37.3	47.0	26	45.6	1.05

The average ultimate strain of the CFRP plates parallel to the CFRP plate direction for ST-1 through ST-3 was 6,213 ìå and that of ST-4 through ST-6 was 6,964 ìå. The 10 percent higher CFRP strain in the misaligned plates was consistent and was due to the misalignment.

Nevertheless, the strain in the concrete parallel to the length of the bridge deck panels was about the same between the two groups of ST specimens. Delamination failure may result from a maximum strain in the concrete parallel to the principle concrete strain rather than from the principle strain in the CFRP plate.

Table 9. Stiffness at 0.4-in. deflection for Group ST specimens

Specimen	Average Unstrengthened (kips/in)	Strengthened (kips/in)	Increase of Stiffness (%)
ST-1	54.1	76.1	41
ST-2		68.0	26
ST-3		67.8	25
Average ST-1 ~ ST-3		70.6	31
ST-4	54.1	69.0	28
ST-5		81.3	50
ST-6		N.A.	N.A.
Average ST-4 ~ ST-6		75.2	39
Average All Specimens	54.1	72.4	34

Table 10. Strains at the maximum load in Sika Carbodur® CFRP plates

Specimen	FS1 (με)	FS2 (με)	FS3 (με)	Average (με)	C.O.V. (%)
ST-1	6,161	5,978	6,210	6,116	2.0
ST-2	5,971	5.649	N.R.	5,810	3.9
ST-3	6,919	6,508	N.R.	6,713	4.3
Average ST-1 ~ ST-3				6,213	
ST-4	6,822	N.R.	7,110	6,966	2.9
ST-5	N.R.	N.R.	N.R.	-	-
ST-6	6,978	6,945	N.R.	6,962	0.3
Average ST-4 ~ ST-6				6,964	

Table 11. Group ST correlation between perceived noises and maximum load

Specimen		First Cracking	Frequent Cracking	At Maximum
ST-1	Load (P, kips)	40.0	46.0	49.6
	Average Strain of CFRP (ε_{CFRP}, $\mu\varepsilon$)	4,153	5,302	6,116
	% of ε_{CFRP} at Failure	68%	87%	100%
ST-2	Load (P, kips)	37.0	40.9	44.7
	Average Strain of CFRP (ε_{CFRP}, $\mu\varepsilon$)	4,204	4,994	5,810
	% of ε_{CFRP} at Failure	72%	86%	100%
ST-3	Load (P, kips)	41.0	45.0	50.0
	Average Strain of CFRP (ε_{CFRP}, $\mu\varepsilon$)	4,968	5,662	6,713
	% of ε_{CFRP} at Failure	74%	84%	100%
Average ST-1 ~ ST-3	Load (P, kips)	39.3	44.0	48.1
	Average Strain of CFRP (ε_{CFRP}, $\mu\varepsilon$)	4,442	5,319	6,213
	% of ε_{CFRP} at Failure	71%	86%	100%
ST-4	Load (P, kips)	35.0	44.0	49.6
	Average Strain of CFRP (ε_{CFRP}, $\mu\varepsilon$)	4,600	6,050	6,966
	% of ε_{CFRP} at Failure	66%	87%	100%
ST-5	Load (P, kips)	38.0	43.0	43.4
	Average Strain of CFRP (ε_{CFRP}, $\mu\varepsilon$)	5,118	N.R.	N.R.
	% of ε_{CFRP} at Failure	-	-	-
ST-6	Load (P, kips)	36.0	43.0	44.7
	Average Strain of CFRP (ε_{CFRP}, $\mu\varepsilon$)	4,740	6,515	6,962
	% of ε_{CFRP} at Failure	68%	94%	100%
Average ST-4 ~ ST-6	Load (P, kips)	36.3	43.3	45.9
	Average Strain of CFRP (ε_{CFRP}, $\mu\varepsilon$)	4,819	6,282	6,964
	% of ε_{CFRP} at Failure	69%	90%	100%
All Specimens	Average Load (P, kips)	37.8	43.6	47.0
	Average Strain of CFRP (ε_{CFRP}, $\mu\varepsilon$)	4,631	5,705	6,513
	% of ε_{CFRP} at Failure	71%	88%	100%

Comparison between Calculated Results and Experimental Results

Moment-curvature and load-deflection responses were computed for each specimen based upon a Todeschini stress block for concrete, the assumption of an elastic-perfectly plastic

response of the steel reinforcement and an elastic response of the CFRP plates. Detailed calculation method is presented in Appendix. It was assumed that plane-sections-remain-plane. The ultimate calculated moment was based upon the average ultimate strain of the CFRP plates recorded in each test. Table 8 lists the calculated maximum load and the ratio of the experimental to calculated ultimate load (P_{exp}/P_{calc}). The ratio P_{exp}/P_{calc} for specimens ST-1 through ST-3 was 1.07 and that for ST-4 through ST-6 was 1.01.

Figure 45 and Figure 46 show the average experimental load-deflection curves for ST-1 through ST-3, and for ST-4 and ST-5, respectively, compared with the calculated load deflection curve. The experimental response agrees very well with the calculated response.

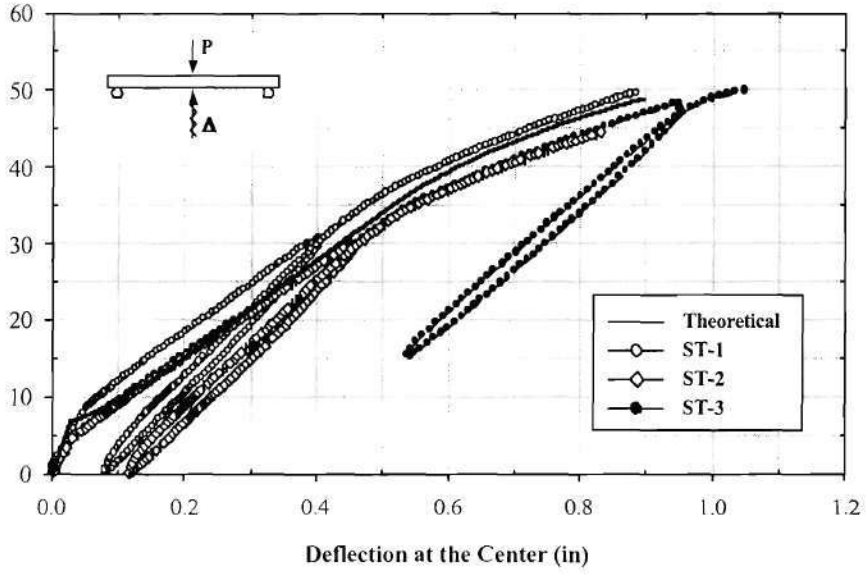

Figure 45. Load-deflection curves for strengthened deck slabs, ST-1 through ST-3

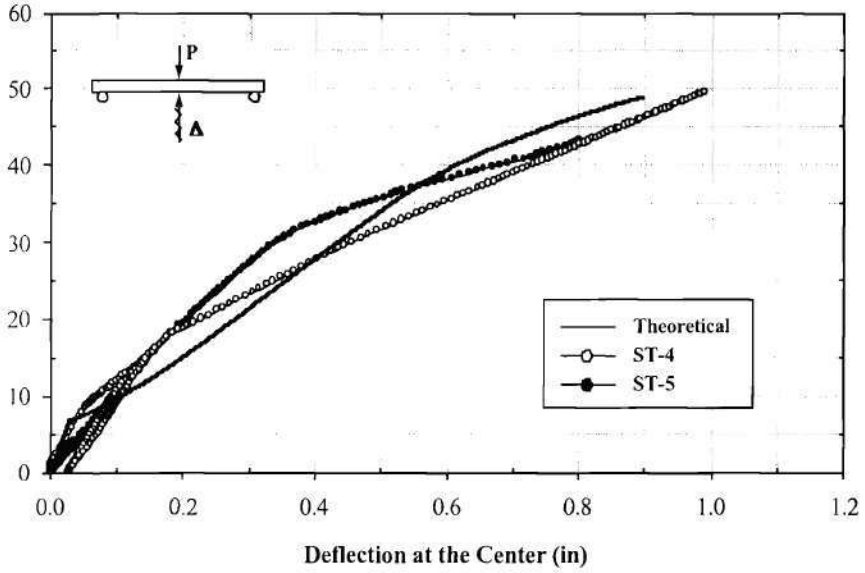

Figure 46. Load-deflection curves for strengthened deck slabs, ST-4 and ST-5

Comparison between Specimens RH-1R through RH-5R and Specimens ST-1 through ST-3: Effect of Strengthening after Cracking

Specimens RH-1R through RH-5R were compared with Specimens ST-1 through ST-3 in order to determine the effect of strengthening the concrete bridge decks before and after cracking and yielding of the reinforcement. Figure 47 plots the average load deflection curve of specimens RH-1R through RH-5R (individual curves shown in Figure 28) and the average load deflection curve of specimens ST-1 through ST-3 (individual curves shown in Figure 45). The unloading cycles have been removed from the ST-1 through ST-3 curve for clarity.

The specimens which were strengthened after cracking (RH-1R through RH-5R) did not show the yield "break" in the load deflection curves until a load of about 45 kips where the specimens strengthened before cracking (ST-1 through ST-3) showed the "break" at about 35 kips. This difference occurred because of the strain hardening of the steel reinforcement in the RH specimens.

The apparent average stiffness of the RH specimens was 69.7 kips/in while that of the ST specimens was 70.6 kips/in. This small difference indicated that the flexural stiffness was not affected by the condition of the bridge deck when the CFRP plates were applied.

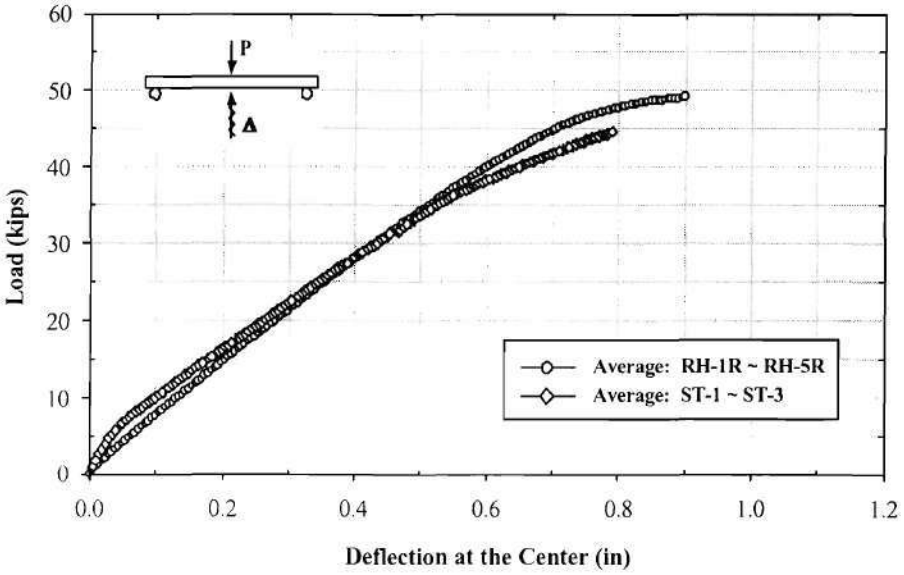

Figure 47. Average load-deflection curves for RH and ST specimens

The average ultimate strength of the strengthened RH specimens was 49.5 kips while that of the ST-1 through ST-3 was 48.1 kips. That the specimens strengthened after cracking and reinforcement yielding had a strength 3 percent greater than those strengthened prior to cracking was due to strain hardening of the reinforcement in the RH specimens. Further, this 3 percent difference is less than the variation in strengths between individual RH specimens and between individual ST specimens. It may be concluded that the benefit of strengthening bridge deck panels with CFRP plates is not affected by when the plates are applied, before or after cracking of the bridge deck.

Comparison of CFRP Failure Strains between RH and ST Specimens

Table 12 shows the average strains in the CFRP plates at the maximum load and at the times when the sounds of first cracking and frequent cracking were heard. The specimens strengthened prior to cracking with the aligned FRP plates (ST-1 through ST-3) had a maximum CFRP strain about 5 percent greater than the maximum strain found in the specimens strengthened after cracking (RH-1R through RH-5R). This 5 percent variation was less than the variation between specimens of each group; therefore, the difference is not considered significant.

Yet, for the specimens strengthened after cracking, the first sounds of delamination cracking occurred at a strain about 53% of the maximum strain while the first cracking sounds of the specimens strengthened before cracking occurred at about 71% of the maximum. It is believed that the precracking did initiate earlier delamination at the crack locations due to non-uniform stresses in the plate-to-concrete bond.

As was stated previously, the strain at which frequent delamination cracking sounds are heard may be considered an effective ultimate strain. These values were nearly identical for the RH and ST specimens. Therefore, a rounded value of 5,000 με may be regarded as the effective ultimate flexural strain.

Table 12. Comparison of CFRP plate strains

Specimen		First Cracking	Frequent Cracking	Maximum
RH-1R through RH-5R	Average (με)	3,151	5,303	5,933
	% of failure strain	53%	89%	100%
ST-1 through ST-3	Average (με)	4,442	5,319	6,213
	% of failure strain	71%	86%	100%
Weighted Average	Average (με)	3,635	5,309	6,038
	% of failure strain	60%	88%	100%

CHAPTER VI CONCLUSIONS AND RECOMMENDATIONS

Shop-manufactured carbon composite plates (e.g. Sika Carbodur®) may be used effectively to flexurally strengthen existing bridge deck panels. A two-inch wide strip provided, on average, a 31 percent increase in flexural capacity per foot width of deck. Increasing the amount of CFRP reinforcement beyond a 2-inch plate per foot width did not increase the flexural capacity. The ultimate capacity of the strengthened panels was not affected by the condition of the deck panel; panels rehabilitated after cracking and yielding of the steel reinforcement demonstrated the same ultimate strength as those strengthened before load was applied. Misalignment of the CFRP plates by as much as 5% did not significantly decrease the ultimate load capacity of the panels. Nevertheless, the load at which yield of the steel reinforcement occurred was less for panels strengthened before cracking than for those strengthened after cracking.

The ultimate strength of all panels occurred after yielding of the bottom layer of steel reinforcement and resulted from delamination of the CFRP plates from the concrete section. The average ultimate strain in the CFRP plate did not depend on the cracked condition of the panel when the plate was epoxy bonded to it. The ultimate strain in the CFRP plates averaged 6,015 με. Based on delamination cracking sounds prior to failure, it is recommended that the effective ultimate strain of the CFRP plates be no larger than 5,000 με. The average ultimate strength increased by 30% after rehabilitation or strengthening. It is important to note that the 30% increase in strength was attained after allowing the epoxy adhesive to cure at least 10 days.

APPENDIX A Test Results for Material Properties

Table 13. Tensile test results for Sika Carbodur® carbon plates

Coupon Number	Width (in)	Thickness (in)	Ultimate Strain (%)	Ultimate Load (kips)	Strength (kips/in)	Modulus, E_x (ksi)
1	0.913	0.051	1.47	17.0	18.6	23713
2	0.927	0.051	1.65	19.4	20.9	23236
3	0.912	0.051	1.43	16.3	17.9	23422
4	0.927	0.051	1.67	19.4	21.0	23486
5	0.926	0.051	1.54	17.9	19.3	23232
6	0.917	0.051	1.47	17.0	18.6	23137
7	0.912	0.051	1.62	18.7	20.5	23068
8	0.917	0.051	1.70	19.5	21.3	23677
9	0.916	0.051	1.57	18.4	20.1	23419
10	0.926	0.051	1.41	16.5	17.8	23410
11	0.927	0.051	1.67	19.5	21.1	23178
12	0.926	0.051	1.85	20.5	22.1	23497
13	0.919	0.051	1.70	19.5	21.3	23242
14	0.916	0.051	1.42	16.2	17.7	23145
15	0.917	0.051	Not recorded	17.9	19.5	23277
Average	0.920	0.051	1.60	18.4	20.0	23343
C.O.V.(%)	0.6	0.0	8.2	7.6	7.4	0.8

Table 14. Shear test results for Sikadur 30® epoxy

Coupon Number	Width (in)	Thickness (in)	Ultimate Strain (%)	Ultimate Load (lb)	Strength (psi)
1	0.464	0.081	0.713	125.6	3343
2	0.443	0.078	0.532	76.8	2224
3	0.439	0.081	1.322	1.322	3854
4	0.447	0.079	0.885	0.885	3823
5	0.460	0.078	0.934	0.934	3492
Average	0.451	0.079	0.877	121.2	3347
C.O.V.(%)	2.4	1.9	33.6	20.8	19.8

APPENDIX B Load-Deflection Response of a Reinforced Concrete Section Based on a Todeschini Stress Block for Concrete

Figure 48 illustrates a reinforced concrete section in which a fiber-reinforced composite (FRC) plate is bonded to the bottom tension surface.

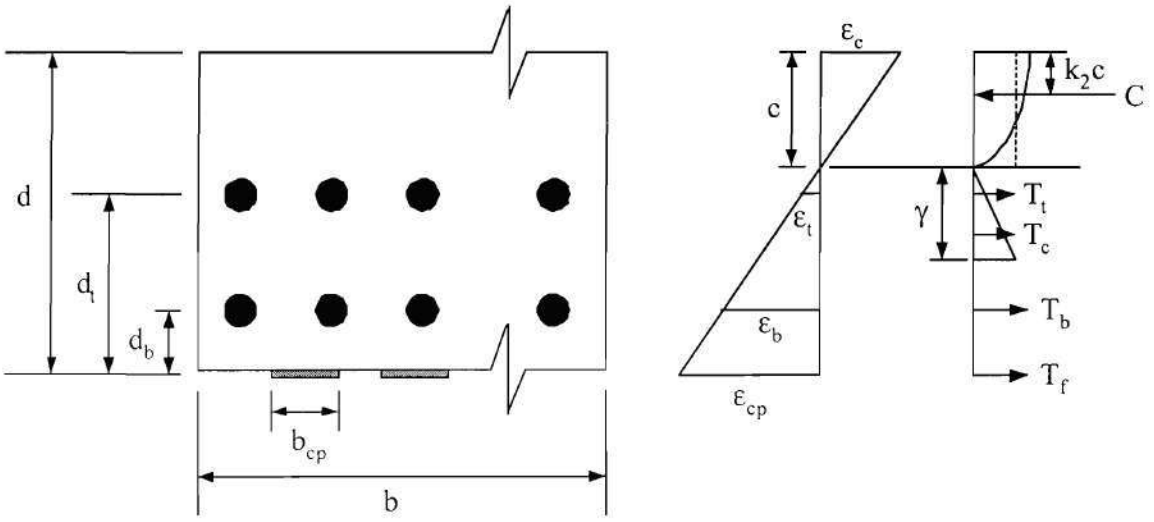

Figure 48. Flexural condition of a bridge deck slab

Under flexure, a linear strain distribution is assumed with ε_c, ε_{cp}, ε_t, and ε_b being the maximum compressive strain in the concrete, the tensile strain in the FRC plate, the strain in the top reinforcing steel, and the strain in the bottom reinforcing steel, respectively; satisfying the following equations:

$$\varepsilon_b = \frac{d - c - d_b}{d - c}\,\varepsilon_{cp}\,, \tag{1}$$

$$\varepsilon_t = \frac{d - c - d_t}{d - c}\,\varepsilon_{cp}\,, \tag{2}$$

$$\varepsilon_c = \frac{c}{d - c}\,\varepsilon_{cp}\,, \tag{3}$$

where c is the distance from the neutral axis to the compressive face of the section.

The concrete compressive stress-strain distribution is assumed to follow the parabolic, Todeschini model shown in Figure 49, expressed in the form:

$$f_c = \frac{2(0.9f_c')(\varepsilon_c/\varepsilon_o)}{1+(\varepsilon_c/\varepsilon_o)^2} \quad , \tag{4}$$

where f_c' is the compressive strength of the concrete and ε_o is the strain, corresponding to the maximum stress, computed from the following equation:

$$\varepsilon_o = 1.71\frac{f_c'}{E_c} \tag{5}$$

E_c is the modulus of elasticity for normal-weight concrete computed from:

$$E_c = 57,000\sqrt{f_c'} \tag{6}$$

The unit for f_c' is in psi.

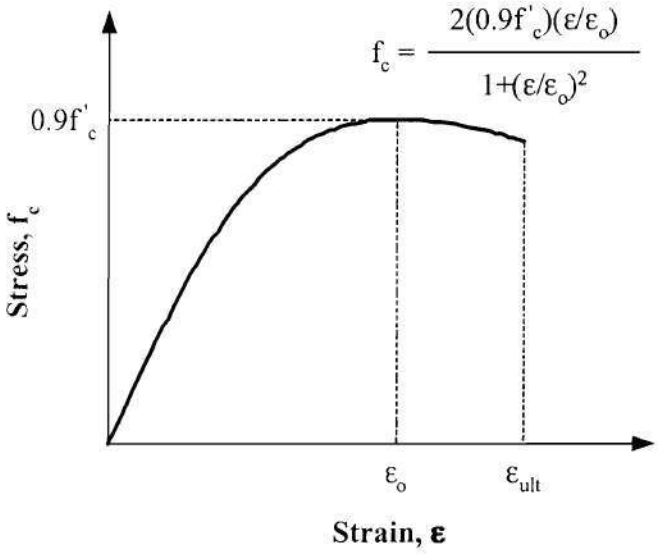

Figure 49. Compressive stress-strain curve for concrete

The compressive force in the concrete can be estimated by using an equivalent rectangular stress block having a depth "c" and an average stress $\beta_1(0.9f_c')$ as illustrated in Figure 48, where β_1 is a factor computed from the following equation:

$$C = b\ c\ \beta_1 (0.9 f_c') \quad , \tag{7}$$

where

$$\beta_1 = \frac{Ln\left[1 + \left(\frac{\varepsilon_c}{\varepsilon_o}\right)^2\right]}{\left(\frac{\varepsilon_c}{\varepsilon_o}\right)} \tag{8}$$

The center of gravity of the compression zone is $k_2 c$ from the compression surface, where k_2 is given in the form:

$$k_2 = 1 - \frac{2\left[\left(\frac{\varepsilon_c}{\varepsilon_o}\right) - tan^{-1}\left(\frac{\varepsilon_c}{\varepsilon_o}\right)\right]}{\left(\frac{\varepsilon_c}{\varepsilon_o}\right)^2 \beta_1} \tag{9}$$

The tensile forces of the steel layers and FRC plates, corresponding to the strains from equations (1) through (3) can be computed as:

$$T_f = A_f E_f \varepsilon_{cp} \, , \tag{10}$$

$$T_b = \begin{cases} A_{sb} E_s \varepsilon_b & \text{if } \varepsilon_b < \varepsilon_y \\ A_{sb} f_y & \text{if } \varepsilon_b \geq \varepsilon_y \end{cases} \quad , \tag{11}$$

$$T_t = \begin{cases} A_{st} E_s \varepsilon_t & \text{if } \varepsilon_t < \varepsilon_y \\ A_{st} f_y & \text{if } \varepsilon_t \geq \varepsilon_y \end{cases} \quad , \tag{12}$$

where A_f, A_{sb}, and A_{st} are areas of CFRP plate, bottom layer steel bar, and top layer steel bar, respectively. E_f and E_s are the elastic moduli of CFRP plate and reinforcing steel, respectively, and f_y and ε_y are the yield strength and yield strain of reinforcing steel, respectively.

The tensile force from the concrete portion in tension can be calculated from:

$$T_c = \begin{cases} \frac{1}{2} b\ \gamma\ E_c\ \varepsilon_{cp} & \text{if } \varepsilon_{cp} < \dfrac{f_r'}{E_c} \\ \frac{1}{2} b\ \gamma\ f_r' & \text{if } \varepsilon_{cp} \geq \dfrac{f_r'}{E_c} \end{cases} \quad , \tag{13}$$

where γ is the distance from the neutral axis to the crack tip computed from:

$$\gamma = \begin{cases} d - c & \text{if } \varepsilon_{cp} < \dfrac{f_r'}{E_c} \\ (d-c)\dfrac{f_r'}{E_c \varepsilon_{cp}} & \text{if } \varepsilon_{cp} \geq \dfrac{f_r'}{E_c} \end{cases}, \tag{14}$$

and f_r' is the modulus of rupture for concrete, which can be computed from:

$$f_r' = 7.5\sqrt{f_c'} \tag{15}$$

Total tension force becomes:

$$T = T_f + T_b + T_t + T_c \tag{16}$$

The distance c can be determined by equating (8) to (16), $C = T$ and solving the resulting equation numerically (e.g. using the Secant iterative technique with a convergence limit of 0.001). The bending moment of the cross-section can be computed from:

$$M = T_f(d - k_2 c) + T_t(d - d_t - k_2 c) + T_b(d - d_b - k_2 c) + T_c\left(c - k_2 c + \frac{2\gamma}{3}\right) \tag{17}$$

The load at midspan becomes:

$$P = \frac{4M}{L}, \tag{18}$$

where L is the span length of the slab.

The deflection at midspan was computed by integrating curvature diagram along the span, as in the form:

$$\delta = \int_0^{\frac{L}{2}} \kappa_x x\, dx, \tag{19}$$

where $\kappa_x = \varepsilon_c / c$ is the curvature corresponding to the moment along the span.